Lynx1 Modulation of Nicotinic Acetylcholine Receptors

Thesis by

Rell Lin Parker

In Partial Fulfillment of the Requirements for the degree

of

Doctor of Philosophy

CALIFORNIA INSTITUTE OF TECHNOLOGY

Pasadena, California

2015

(Defended July 11th 2014)

ACKNOWLDEGMENTS

My graduate school career and dissertation would not have been possible without my partner and supporter, Jesse. The great reward of being at Caltech has been the opportunity to live in Los Angeles and be close to my GMa. She has kept me full with sushi and has been a constant inspiration. I aspire to her drive, sense of adventure, and ability to be friends with everyone. It has also been wonderful to be close to the rest of my family in Los Angeles: Lisa, Michael, Samantha, Greg, Olivia, Zachary, Johnny, Annemarie, Alexis, Victoria, Megan, and Bax. Thanks to the rest of my family, particularly my parents for their support. Thanks to GPT for his constant interest in my scientific pursuits.

Thank you to Henry Lester for his guidance and support. I appreciate the opportunity to learn electrophysiology under his expert tutelage. Thank you to all of the members of the Lester lab, past and present, that have helped me along the way: Purnima, Bruce, Julie, Ryan, Andrew, Cheng, Rachel, Chris, Brandon, Weston, Sheri, Rahul, Elisha, Jonathan, Doreen, Mark, and Atsuko. Thank you in particular to Julie, for guiding me during my formative years and teaching me many things. Thanks to my Caltech family: Eloisa, Michelle, Ying, Shawna, Crystal, and Teagan. It has been a pleasure to go through this experience with you all by my side. Shawna and Crystal, I was so lucky to have you both to help me navigate graduate school and the Lester lab.

Thank you to my committee: David Chan, Markus Meister, and David Prober. Thank you also to Paul Patterson, former committee member. Thank you all for your helpful comments and guidance. Our meetings have helped me immensely.

Thank you to the rest of my support system at Caltech. Thank you to Felicia Hunt for her encouragement and advice. Special thanks to Liz Ayala for always helping and having time to talk. Thanks to Bruce Hay for his advice. Thank you to Portia Harris for helping all of the women on campus. Thank you to Jennifer Costanza for her help with managing my mouse colonies. Thank you to the animal technicians, Joaquin, Jorge, Syed, Lorena, Ingrid, and Sidali, who have all taken care of my animals.

Special thanks to Jenny, my dog. Thanks for always greeting me with a wagging tail, forcing me to go on walks, and always making me laugh.

ABSTRACT

Nicotinic receptors are the target of nicotine in the brain. They are pentameric ion channels. The pentamer structure allows many combinations of receptors to be formed. These various subtypes exhibit specific properties determined by their subunit composition. Each brain region contains a fixed complement of nicotinic receptor subunits. The midbrain region is of particular interest because the dopaminergic neurons of the midbrain express several subtypes of nicotinic receptors, and these dopaminergic neurons are important for the rewarding effects of nicotine. The α6 nicotinic receptor subunit has garnered intense interest because it is present in dopaminergic neurons but very few other brain regions. With its specific and limited presence in the brain, targeting this subtype of nicotinic receptor may prove advantageous as a method for smoking cessation. However, we do not fully understand the trafficking and membrane localization of this receptor or its effects on dopamine release in the striatum. We hypothesized that lynx1, a known modulator of other nicotinic receptor subtypes, is important for the proper function of α6 nicotinic receptors. lynx1 has been found to act upon several classes of nicotinic receptors, such as α4β2 and α7, the two most common subtypes in the brain. To determine whether lynx1 affects α6 containing nicotinic receptors we used biochemistry, patch clamp electrophysiology, fast scan cyclic voltammetry, and mouse behavior. We found that lynx1 has effects on α6 containing nicotinic receptors, but the effects were subtle. This thesis will detail the observed effects of lynx1 on α6 nicotinic receptors.

TABLE OF CONTENTS

LIST OF FIGURES

NOMECLATURE

*. denotes a nicotinic receptor containing the starred subunit, other subunits not specified

α6L9'S. BAC transgenic mice containing a point mutation in the 9' position of the pore lining domain of α6 nicotinic receptor subunit

α-CTX MII. alpha-conotoxin MII, a blocker of α6* nicotinic receptors

DA. Dopamine

COIP. Co-immunoprecipitation

CPP. Conditioned Place Preference

EPSC. Excitatory Post Synaptic Potential

FSCV. Fast Scan Cyclic Voltammetry

IPSC. Inhibitory Post Synaptic Potential.

lynx1KO. lynx1 knockout mouse

nAChRs. nicotinic acetylcholine receptors

nic. nicotine

PPI. Paired Pulse Inhibition

SNc. Substantia Nigra pars compacta

VTA. Ventral Tegmental Area

Introduction

Cholinergic Signaling and Nicotinic Receptors

The neurotransmitter acetylcholine defines the cholinergic system. Acetylcholine acts at both the nicotinic and muscarinic ligand gated receptors. Muscarinic receptors are G-protein coupled receptors, while nicotinic receptors are ion channels. Nicotinic receptors are pentameric cation channels activated by nicotine in addition to the endogenous ligand acetylcholine. Nicotinic receptors at the neuromuscular junction are responsible for muscle contraction.

Neuronal nicotinic receptor subunits are comprised of α2-10 and β2-4 and can be homomeric or heteromeric in composition. α7 receptors are the most common homomeric receptors, while α4β2 are the most common heteromeric receptors. Nicotinic receptors are spread throughout the brain, and they act to modulate other neurotransmitter systems (Dani and Balfour, 2011).

The rewarding effects of tobacco are mediated by nicotine acting on dopaminergic neurons. These dopaminergic neuron cell bodies are in the ventral tegmental area (VTA) and project to the nucleus accumbens (NAc). They form the mesolimbic system. These dopaminergic neurons express a variety of nicotinic receptor subtypes (Grady et al., 2007; De Biasi and Dani, 2011). Application of nicotine changes the firing rate of dopaminergic neurons, which may be a cellular mechanism of addiction (Mameli-Engvall et al., 2006). Recent studies have shown that activation of nicotinic receptors on dopaminergic neurons via synchronized activation of cholinergic interneurons is sufficient to cause DA release (Cachope et al., 2012; Threlfell et al., 2012).

Nicotine addiction is a serious public health issue. It has been 50 years since the Surgeon General's report linked tobacco to disease (Schroeder and Koh, 2014). 50 years of knowledge and research has reduced but has not been able to eliminate mortality due to tobacco usage. The most recent data shows that 12% of deaths among adults over the age of 30 are attributable to tobacco (WHO Global Report: Mortality Attributable to Tobacco). WHO estimated that 5 million people died in 2004 from direct tobacco use. Much more needs to be done to reduce the levels of nicotine addiction, and therefore the morbidity and mortality due to tobacco.

The α6 Nicotinic Receptor Subunit

α6 nicotinic receptors are a particularly interesting nicotinic receptor subunit. The expression of α6 is limited to a few brain regions: the dopaminergic neurons of the SNc and VTA, the superior colliculus, and a population of retinal ganglion cells (Le Novere et al., 1996; Whiteaker et al., 2000; Champtiaux et al., 2003). Their localization in dopaminergic neurons in particular suggests that this subtype of nicotinic receptor is important in nicotine addiction. α6 knockout mice do not self administer nicotine, and the restoration of the α6 nicotinic receptor subunit to the VTA dopaminergic neurons restores self administration behavior (Pons et al., 2008). This indicates the necessity of α6* nicotinic receptors for addiction. Mice with hypersensitive α6 nicotinic receptor subunits exhibit an increased response to nicotine. They are hyperactive with low doses of nicotine, and they exhibit conditioned place preference to low doses of nicotine as well (Drenan et al., 2008; Drenan et al., 2012). These studies provide evidence that activation of α6* nicotinic receptors is sufficient for behavioral responses to nicotine.

The limited expression of this subtype makes it an appealing drug target (Quik and McIntosh, 2006; Quik et al., 2011). While α4β2* subtypes are also important in nicotine addiction, they are highly expressed throughout many different regions of the brain and are the most common

nicotinic receptor in the brain (Tapper et al., 2004). The risk of off-target effects makes α4β2 nicotinic receptors a less appealing drug target. Although they only represent about half of the total number of nicotinic receptors on dopaminergic neurons, α6* nicotinic receptors appear to have a much greater functional contribution to mesolimbic dopamine release (Perez et al., 2009; Quik et al., 2011). Fast scan cyclic voltammetry measurements in the NAc of C57BL/6 mouse brain slices were used to measure dopamine release in the NAc. Measurements made using either α-CTXMII (blocking α6* receptors) or DHβE (blocking β2* receptors) were reduced by the same amount (Quik et al., 2011). This indicates that the majority of evoked dopamine release in the NAc is mediated by α6* receptors.

The α6* nicotinic receptor is important in nicotine addiction, but unfortunately it is very difficult to study in heterologous systems (Letchworth and Whiteaker, 2011). For this reason, our lab has developed a mouse model that allows one to more easily isolate the effect of the α6* containing receptors. To generate hypersensitive receptors, a single amino acid in the pore domain, L9'S , was mutated (Drenan et al., 2008; Drenan and Lester, 2012). Mice expressing these α6L9'S nicotinic receptors exhibit hyperactivity when introduced to new environments and are also hyperactive at night (Drenan et al., 2008). Additionally, recordings from the VTA, NAc, and SNc of α6L9'S mice confirm that hypersensitive α6* receptors are expressed in these regions (Drenan et al., 2008). This mouse model provided a basis for the studies of α6* nicotinic receptors conducted in this thesis.

lynx1 as a Modulator of Nicotinic Receptors

lynx1 is a protein that can bind to nicotinic receptors. It has structural similarity to α-bungarotoxin, a snake venom toxin that is an inhibitor of α7 nicotinic receptors (Miwa et al., 1999; Lyukmanova et al., 2011). However, lynx1 and its family members, which comprise the

ly-6/uPAR superfamily, are endogenously expressed in the brain to act as regulators of nicotinic acetylcholine receptor function (Miwa et al., 1999; Miwa et al., 2011; Miwa et al., 2012). Lynx1 is a GPI anchored protein, which means that it is tethered to the outer leaflet of the cell membrane (Miwa et al., 1999; Miwa and Walz, 2012). lynx1's GPI anchor and similarity to α-bungarotoxin indicate that it interacts with the external portion of nicotinic receptors (Lyukmanova et al., 2013).

lynx1 can modulate several subtypes of nicotinic receptors, which are known to include α4β2 and α7 (Miwa et al., 1999; Ibanez-Tallon et al., 2002; Miwa et al., 2011). Several studies of lynx1 have been conducted in lynx1 knockout mice, revealing changes at both the receptor and circuit level (Miwa et al., 2006; Miwa et al., 2011). Patch clamp electrophysiological recordings were performed in the medial habenula, a brain region with a high concentration of nicotinic receptors. The lynx1 knockout mice (lynx1KO) showed an increased peak response to nicotine. These cells also exhibited a shift to the left in the concentration-response curve (Miwa et al., 2006). These two results suggest that lynx1KO leads to an increase in nicotinic receptor activity in response to nicotine. While we do not know exactly which nicotinic receptors were recorded from in the medial habenula, it was likely a combination of α4β2, with possibly α3 and β4 receptors also present (Lester Lab, unpublished data). The shift in the dose response curve indicates an increase in sensitivity to nicotine, and the increased peak response also indicates that the receptors are hypersensitive in the absence of lynx1 (Miwa et al., 2006).

Synaptic and circuit level effects have also been studied in the lynx1KO mice. In the hippocampus, there is a difference in the paired pulse response when CA3 is stimulated and field potential recordings are made in CA1 (Miwa et al., 2006). With a time interval of greater than 50 ms, the paired pulse ratio in the lynx1KO is significantly decreased compared to lynx1WT. This suggests that the first pulse is depleting the synapse in the lynx1KO, which is consistent with the

finding of hypersensitive nicotinic receptors in the lynx1KO.

In the lynx1KO mice, the critical period for vision is extended, and the visual system retains its plasticity into adulthood (Morishita et al., 2010). This is an example of the circuit level changes that occur in the lynx1KO mice. Short term monocular deprivation in adult lynx1KO mice is sufficient to affect ocular dominance. lynx1 normally turns on late in development to dampen acetylcholine signaling, which causes the decrease in plasticity that denotes the end of the critical period for vision. This hypothesis was confirmed by adding an acetycholinesterase inhibitor to increase cholinergic signaling in adult wild-type mice, which increased cholinergic signaling and re-opened the critical period. The level of cholinergic signaling regulates the excitatory-inhibitory balance of the primary visual cortex, which determines the level of plasticity (Morishita et al., 2010). lynx1 appears to control the setpoint of cholinergic signaling in the visual cortex during development, to determine the level of plasticity.

Another consequence of lynx1KO is an increase in associative learning (Miwa et al., 2006). Using fear conditioning as a measure of learning, the lynx1KO mice exhibited increased cued fear conditioning, but did not exhibit increased contextual fear conditioning compared to lynx1WT mice. Cholinergic circuits in the primary auditory cortex are essential for the development of fear conditioning behavior (Letzkus et al., 2011). Local application of nicotinic receptor antagonists mecamylamine and methyllycacontine into the auditory cortex were shown to reduce fear levels during conditioning (Letzkus et al., 2011). In contrast to the effects of the receptor antagonists, lynx1KO mice appear to have increased cholinergic signaling in this circuit that enhances their cued fear conditioning.

lynx1 has been studied in a variety of different brain regions, from the level of individual receptor subunits to behavioral outputs in the lynx1KO mice. It has consistently been found that removal

of lynx1 increases the activation of nicotinic receptors. However, it is not known whether lynx1 can interact with α6 nicotinic receptors (Miwa et al., 2011). One of the primary goals of my research has been to determine whether lynx1 affects α6 nicotinic receptors. These studies are detailed in Chapters 1 and 2. Additionally, I have done a variety of other studies on lynx1. A summary of some of these experiments is provided in Chapter 3.

References

Cachope R, Mateo Y, Mathur BN, Irving J, Wang H-L, Morales M, Lovinger DM, Cheer JF (2012) Selective activation of cholinergic interneurons enhances accumbal phasic dopamine release: setting the tone for reward processing. Cell Reports 2:33-41.

Champtiaux N, Gotti C, Cordero-Erausquin M, David DJ, Przybylski C, Lena C, Clementi F, Moretti M, Rossi FM, Le Novere N, McIntosh JM, Gardier AM, Changeux JP (2003) Subunit composition of functional nicotinic receptors in dopaminergic neurons investigated with knock-out mice. J Neurosci 23:7820-7829.

Dani JA, Balfour DJK (2011) Historical and current perspective on tobacco use and nicotine addiction. Trends in neurosciences 34:383-392.

De Biasi M, Dani JA (2011) Reward, addiction, withdrawal to nicotine. Annual review of neuroscience 34:105-130.

Drenan RM, Lester HA (2012) Insights into the neurobiology of the nicotinic cholinergic system and nicotine addiction from mice expressing nicotinic receptors harboring gain-of-function mutations. Pharmacol Rev 64:869-879.

Drenan RM, Engle S, Lester HA, McIntosh JM, Brunzell DH (2012) Activation of α6β2* nicotinic acetylcholine receptors is sufficient for nicotine reward. In: Society for Neuroscience. New Orleans, LA: Program No. 455.03 Neuroscience Meeting Planner.

Drenan RM, Grady SR, Whiteaker P, McClure-Begley T, McKinney SR, Miwa J, Bupp S, Heintz N, McIntosh JM, Bencherif M, Marks MA, Lester HA (2008) *In Vivo* Activation of Midbrain Dopamine Neurons via Sensitized, High-Affinity α6* Nicotinic Acetylcholine Receptors. Neuron 60:123-136.

Grady SR, Salminen O, Laverty DC, Whiteaker P, McIntosh JM, Collins AC, Marks MJ (2007) The subtypes of nicotinic acetylcholine receptors on dopaminergic terminals of mouse striatum. Biochem Pharmacol 74:1235-1246.

Ibanez-Tallon I, Miwa JM, Wang HL, Adams NC, Crabtree GW, Sine SM, Heintz N (2002) Novel modulation of neuronal nicotinic acetylcholine receptors by association with the endogenous prototoxin lynx1. Neuron 33:893-903.

Le Novere N, Zoli M, Changeux JP (1996) Neuronal nicotinic receptor a6 subunit mRNA is selectively concentrated in catecholaminergic nuclei of the rat brain. Eur J Neurosci 8:2428-2439.

Letchworth SR, Whiteaker P (2011) Progress and challenges in the study of α6-containing nicotinic acetylcholine receptors. Biochemical pharmacology 82:862-872.

Letzkus JJ, Wolff SBE, Meyer EMM, Tovote P, Courtin J, Herry C, Lüthi A (2011) A disinhibitory microcircuit for associative fear learning in the auditory cortex. Nature 480:331-335.

Lyukmanova EN, Shulepko MA, Buldakova SL, Kasheverov IE, Shenkarev ZO, Reshetnikov RV, Filkin SY, Kudryavtsev DS, Ojomoko LO, Kryukova EV, Dolgikh DA, Kirpichnikov MP, Bregestovski PD, Tsetlin VI (2013) Water-soluble LYNX1 residues important for interaction with muscle-type and/or neuronal nicotinic receptors. The Journal of biological chemistry 288:15888-15899.

Lyukmanova EN, Shenkarev ZO, Shulepko MA, Mineev KS, D'Hoedt D, Kasheverov IE, Filkin SY, Krivolapova AP, Janickova H, Dolezal V, Dolgikh DA, Arseniev AS, Bertrand D, Tsetlin VI, Kirpichnikov MP (2011) NMR structure and action on nicotinic acetylcholine receptors of water-soluble domain of human lynx1. J Biol Chem 288:15888-15899.

Mameli-Engvall M, Evrard A, Pons S, Maskos U, Svensson TH, Changeux JP, Faure P (2006) Hierarchical control of dopamine neuron-firing patterns by nicotinic receptors. Neuron 50:911-921.

Miwa JM, Walz A (2012) Enhancement in motor learning through genetic manipulation of the Lynx1 gene. PloS one 7:e43302.

Miwa JM, Freedman R, Lester HA (2011) Neural systems governed by nicotinic acetylcholine receptors: emerging hypotheses. Neuron 70:20-33.

Miwa JM, Lester HA, Walz A (2012) Optimizing cholinergic tone through lynx modulators of nicotinic receptors: implications for plasticity and nicotine addiction. Physiology 27:187-199.

Miwa JM, Ibanez-Tallon I, Crabtree GW, Sanchez R, Sali A, Role LW, Heintz N (1999) lynx1, an endogenous toxin-like modulator of nicotinic acetylcholine receptors in the mammalian CNS. Neuron 23:105-114.

Miwa JM, Stevens TR, King SL, Caldarone BJ, Ibanez-Tallon I, Xiao C, Fitzsimonds RM, Pavlides C, Lester HA, Picciotto MR, Heintz N (2006) The Prototoxin lynx1 Acts on Nicotinic Acetylcholine Receptors to Balance Neuronal Activity and Survival In Vivo. Neuron 51:587-600.

Morishita H, Miwa J, Heintz N, Hensch T (2010) Lynx1, a cholinergic brake, limits plasticity in adult visual cortex. Science 330:1238-1240.

Perez XA, O'Leary KT, Parameswaran N, McIntosh JM, Quik M (2009) Prominent Role of α3/α6 β2* nAChRs in Regulating Evoked Dopamine Release in Primate Putamen: Effect of Long-Term Nicotine Treatment. 75:938-946.

Pons S, Fattore L, Cossu G, Tolu S, Porcu E, McIntosh JM, Changeux JP, Maskos U, Fratta W (2008) Crucial role of α4 and α6 nicotinic acetylcholine receptor subunits from ventral tegmental area in systemic nicotine self-administration. J Neurosci 28:12318-12327.

Quik M, McIntosh JM (2006) Striatal a6* nicotinic acetylcholine receptors: potential targets for Parkinson's disease therapy. J Pharmacol Exp Ther 316:481-489.

Quik M, Perez XA, Grady SR (2011) Role of α6 nicotinic receptors in CNS dopaminergic function: Relevance to addiction and neurological disorders. Biochem Pharmacol.

Schroeder SA, Koh HK (2014) Tobacco Control 50 Years After the 1964 Surgeon General's Report. JAMA : the journal of the American Medical Association 311:141-143.

Tapper AR, McKinney SL, Nashmi R, Schwarz J, Deshpande P, Labarca C, Whiteaker P, Marks MJ, Collins AC, Lester HA (2004) Nicotine activation of α4* receptors: sufficient for reward, tolerance and sensitization. Science 306:1029-1032.

Threlfell S, Lalic T, Platt NJ, Jennings KA, Deisseroth K, Cragg SJ (2012) Striatal dopamine release is triggered by synchronized activity in cholinergic interneurons. Neuron 75:58-64.

Whiteaker P, McIntosh JM, Luo S, Collins AC, Marks MJ (2000) ^{125}I-α-conotoxin MII identifies a novel nicotinic acetylcholine receptor population in mouse brain. Molecular Pharmacology 57:913-925.

Chapter 1

Lynx1 knockout reduces the function of α6* nicotinic receptors

*This chapter is being prepared for submission as a manuscript to PLOS One

Authors

Rell L Parker[1]; Heidi C O'Neil[2]; Andrew D Steele[3]; Xiomara A Perez[4]; Maryka Quik[4]; Charles R Wageman[2]; Ryan M Drenan[5]; Mike J Marks[2]; Sharon R Grady[2]; Julie M Miwa[6]; Henry A Lester[1]

Affiliations: [1]Division of Biology and Biological Engineering, California Institute of Technology, Pasadena, CA; [2]Institute for Behavioral Genetics, University of Colorado Boulder, Boulder, CO; [3]Department of Biological Sciences, Cal Poly Pomona, Pomona, CA; [4]Center for Health Sciences, SRI International, Menlo Park, CA; [5]Department of Medicinal Chemistry and Molecular Pharmacology, Purdue University, West Lafayette, IN; [6]Department of Biological Sciences, Lehigh University, Bethlehem, PA

Abstract

The α6 nicotinic receptor subunit is considered to be an attractive drug target for nicotine addiction. With its specific and limited presence in the brain, targeting this subtype of nicotinic receptor may prove advantageous over other subtypes of nicotinic receptors. However, we do not fully understand the trafficking and membrane localization of this receptor or its effects on dopamine release in the striatum. We hypothesized that lynx1, a known modulator of other nicotinic receptor subtypes, is important for the proper function of α6 nicotinic receptors. We used transgenic mice that contain a hypersensitive mutation in the α6 subunit — α6L9'S mice —

and lynx1 knockout mice. These mouse models allowed us to probe the effects of lynx1 on α6 containing nicotinic receptors. We extracted synaptosomes from these mice to determine epibatidine binding, rubidium efflux, and nicotine mediated DA release. lynx1KO reduced the α6 component of rubidium efflux and nicotine mediated DA release. No effect of lynx1KO was detected in slice electrophysiology experiments conducted in substantia nigra pars compacta, or in fast scan cyclic voltammetry experiments completed in dorsal striatal slices. It appears that the effects of lynx1 on α6 containing nicotinic receptors are subtle and regionally specific.

Introduction

Nicotinic receptors are essential for many aspects of normal brain function, but their most important public health relevance is their role in nicotine addiction. Nicotine addiction causes approximately 12% of worldwide deaths in people over 30 years of age (WHO Global Report: Mortality Attributable to Tobacco). The high rate of death due to nicotine addiction makes it a moral imperative to find highly effective methods of nicotine cessation. In the search for a drug for nicotine cessation, one particular subclass of nicotinic acetylcholine receptors, the α6 subunit, has garnered intense interest as a drug target (Quik et al., 2011; Brunzell, 2012). Studies have shown that α6 containing (α6*) nicotinic receptors are necessary for the rewarding effects of nicotine (Pons et al., 2008; Jackson et al., 2009). The α6* nicotinic receptor is highly localized in the brain and is restricted to few locations in the brain, namely the dopaminergic neurons of the VTA and SNc, the retina, parts of the superior colliculus, and the medial habenula (Whiteaker et al., 2000; Grady et al., 2007; Mackey et al., 2012). The localization of α6* receptors to the DA neurons of the VTA and SNc suggests that drugs targeting this specific subtype could change the nicotinic receptor response in DA neurons, which mediate nicotine reward, with minimal risk of affecting other brain regions (Exley et al., 2008; Jackson et al., 2009; Brunzell, 2012).

One way to study the α6 nicotinic receptor subunit is to put a gain-of-function mutation in the pore lining domain. This produces hypersensitive receptors that are more sensitive to nicotine, demonstrated with a shift to the left in the dose-response curve (Tapper et al., 2004; Drenan and Lester, 2012). Mice containing the α6L9'S mutation are BAC transgenic mice that express several copies of the α6 gene, which has been modified by a L9'S mutation (Drenan et al., 2008). Several studies have used these mice to understand the function of the α6* nicotinic receptor function in vivo (Drenan et al., 2010; Powers et al., 2013; Wang et al., 2013). Mice with α6L9'S nicotinic receptors exhibit several phenotypes due to overactivation of α6* nicotinic receptors in dopaminergic neurons of the VTA and SNc (Drenan et al., 2008). We chose to use these mice to determine whether lynx1KO affects α6* nicotinic receptors, which would result in either reducing or augmenting the known phenotypes of the α6L9'S mice.

We asked whether lynx1 regulates α6* nicotinic receptor expression and function. Previous studies demonstrate that lynx1 is capable of modulating several classes of nicotinic receptors, including α4β2 and α7 nicotinic receptor subtypes (Miwa et al., 1999; Ibanez-Tallon et al., 2002; Miwa et al., 2006). lynx1 can act as a brake on nicotinic receptor function by casing a shift to the left of concentration-response curves, inhibiting the maximal receptor response, and increasing the rate of desensitization (Miwa et al., 1999; Ibanez-Tallon et al., 2002; Miwa et al., 2006; Morishita et al., 2010). None of the previous studies of lynx1 function examined whether lynx1 produces effects on α6* nicotinic receptors. This study utilizes biochemical approaches, along with electrophysiology and behavior in lynx1KO and α6L9'S mice, to determine whether lynx1 regulates α6* nAChRs. We found that there are effects of lynx1 on α6* nicotinic receptor localization and function. However, the effects detected were very specific and did not result in significant behavioral effects.

Materials and Methods

Cell Culture, western blot, and co-immunoprecipitation:

HEK293 and Neuro2a (N2a) cells were obtained from ATCC and were maintained with DMEM, Sodium Pyruvate, Pen-Strep antibiotics, and 10% FBS (HEK293) or 45% DMEM, 45% Optimem, 10% FBS, and Pen-Strep antibiotics (N2a). Cells were transfected using Express-Fect (Denville Scientific) and plasmids pCI-neo-α6YFP, pCI-neo-β2WT, and pc-DNA3.1-lynx1. For the Co-immunoprecipitation, HEK293 cells were transfected. 48 hours post transfection, cells were harvested by scraping with PBS, and spun down at 4000 rpm for 4 minutes for collection. Cells were lysed using ice-cold extraction buffer, pH 7.4, containing 50 mM Tris, 50 mM NaCl, 1% NP40, 1 mM EDTA, 1 mM EGTA. The solution was supplemented with fresh 1% P8340 and 4 mM PMSF for each experiment. The cells were pipetted up and down in the extraction buffer 20-30 times and then allowed rest on ice for 5-10 min. Following that, they were centrifuged at 14000 rpm for 5 minutes at 4° C. The supernatant was transferred to a new tube, with 50 µL of the supernatant being set aside for the input lane. Then, dynabeads that had been pre-coated with antibody (Invitrogen cat #11122) were added. To bind the antibody to the protein A dynabeads, (Invitrogen) 5 µg of antibody was diluted into 200 µL PBS with 0.02% Tween-20, and this was mixed with 50 µL of beads. The antibody and bead mixture was rotated on a mixer for 20 minutes at room temperature to allow the antibody to bind and was then washed 1 time with PBS with 0.02% Tween-20 before the cell supernatant was added. The supernatant was mixed with the antibody bound beads for 1 hour at room temperature. The beads were then washed 3 times with PBS. 20 µL of 1x Lammeli buffer (Bio-Rad) was added to the beads, which were then heated to 70° C for 10 minutes. The sample buffer was then ready to be loaded on to the gel for western blot.

The samples were loaded onto a 4-10% gradient gel (Bio-Rad) and electrophoresed for 1.5 hours at 100 V. The protein was transferred to nitrocellulose membrane using a semi-dry transfer system and 3 buffer system for 15 minutes at 15 V. The membrane was blocked with 5% milk for 1 hr, then probed with primary goat anti-lynx1 antibody (Santa Cruz) at 1:500 in 5% milk overnight at 4° C. The top part of the membrane was probed with the same rabbit anti-GFP antibody at 1:500 overnight. The secondary antibodies used were goat anti-rabbit at 1:5000 for one hour and donkey anti goat at 1:2000 for two hours. Western blots were imaged either using anti-HRP secondary antibodies and film or using fluorescent secondary antibodies and a Li-Cor imaging system.

Cell electrophysiology:

Cells were maintained and transfected as described above, but for electrophysiology they were plated at a lower density onto glass coverslips. 48 hours post-transfection, the cells were transferred to the 32° C recording chamber, where they were perfused with oxygenated (95% O_2 / 5% CO_2) ACSF. The ACSF consists of (in mM): 124 NaCl, 3 KCl, 1.25 NaH_2PO_4, 26 $NaHCO_3$, 10 glucose, 1.3 $MgSO_4$, and 2.5 $CaCl_2$ (Nashmi et al., 2007). Cells were visualized with a UV lamp to determine which had been transfected with α6GFP, and a whole cell patch clamp configuration was obtained. Cells were puffed with nicotine using a picosprizter, and the response was recorded.

Animals:

All animal experiments were conducted in accordance with the *Guide for Care and Use of Laboratory Animals*, and protocols were approved by the Institutional Animal Care and Use Committee at Caltech (Protocol 1386-13) or the University of Colorado Boulder. Mice used for experiments were generated from breeding pairs where both parents were heterozygous for the

lynx1KO allele and where one of the parents had the BAC transgene containing the α6L9'S mutation (Miwa et al., 2006; Drenan et al., 2008). Animals were group housed, except for immediately before and during behavioral experiments. The animals had free access to food and water and were on a 13 h dark: 11 h light cycle. During behavioral experiments, when conditions allowed, mice were used for novel environment experiments, then AMBA, and finally for single injection of nicotine.

Slice electrophysiology: Mice used for midbrain recordings are P17 to P25. All animals were genotyped before and after the experiment (animal numbers: 11 lynx1WT α6L9'S, 13 lynx1KO α6L9'S, 8 lynx1WT, 8 lynx1KO). Animals were euthanized with CO_2 gas, then subjected to cardiac perfusion with an oxygenated (95 % O_2 / 5 % CO_2) ice-cold glycerol-substituted ACSF containing (in mM): 250 glycerol, 2.5 KCl, 1.2 NaH_2PO_4, 26 $NaHCO_3$, 11 glucose, 1.3 $MgCl_2$, and 2.4 $CaCl_2$. The animals were then decapitated and the brain was dissected out and mounted on a vibratome in the ice-cold glycerol ACSF. 250 μM coronal sections were made using a vibratome (DTK-1000; Ted Pella, Redding, CA). Slices were allowed to recover for 1 hour in regular ACSF bubbled with 95% O_2 / 5% CO_2 at 32° C, then moved to room temperature. The ACSF consists of (in mM): 124 NaCl, 3 KCl, 1.25 NaH_2PO_4, 26 $NaHCO_3$, 10 glucose, 1.3 $MgSO_4$, and 2.5 $CaCl_2$ (Nashmi et al., 2007). After 15 minutes at room temperature the slices were put into fresh room temperature ACSF. Recordings were made in a chamber perfused with ACSF at 32° C, bubbled with 95% O_2 / 5% CO_2, at a rate of 1-2 mL/min. The internal solution in mM consisted of 135 potassium gluconate, 5 EGTA, 10 HEPES, 2 $MgCl_2$, 0.5 CaCl2, 3 Mg-ATP, and 0.2 GTP. The slices were visualized with an upright microscope (BX50WI, Olympus) and near-infrared illumination. Recordings were made from the VTA or SNc, and a picture was taken of each cell recorded from to verify location. We tested for I_h and measured the firing rate to determine that we were indeed recording from a dopaminergic neuron. Patch pipettes were made

using a programmable microelectrode puller (P-87; Sutter Instrument Co.; Novato, CA) and pipette resistances were 4-8 mΩ. Recordings were made with an Axon Multiclamp 700A Amplifier and recorded using Clampex 10, both from Molecular Devices, Sunnyvale, CA. Data was sampled at 5 kHz and low-pass filtered at 2 kHz. The holding potential was -65 mV, and the puffer pipette was moved to within one cell length of the cell by a piezoelectric controller (Burleigh Instruments; Fishers Park, NY). Over a period of 1.4 s, there was a 100 ms pause, a puff of 200 ms drug was applied using a picospritzer, and then the puffer pipette was retracted over 360 ms. Data was analyzed using Clampfit 10, also from Molecular Devices.

Fast Scan Cyclic Voltammetry (FSCV): Electrodes were fabricated using carbon fiber (7 μM, unsized from Goodfellow) and glass without filament from Sutter. One carbon fiber was pulled through a glass micropipette. This was then pulled into two eletrodes on a Sutter Puller (P-87). The carbon fibers were trimmed, and the electrodes dipped into epoxy for 7 minutes and then quickly rinsed in acetone. Electrodes were baked overnight at 80° C to cure the epoxy. Usually, the carbon fiber was trimmed once more just before use. The carbon fiber was placed in the dorsal striatum, just below the surface of the slice. The animals used in these experiments were 18-27 weeks old (Animal numbers: 10 lynx1WT α6L9'S, 7 lynx1KO α6L9'S). Slices were prepared in a similar fashion as done with electrophysiology, except the slices were 300 μM thick and were taken from the striatum. Recordings were made with an Axon Multiclamp 700B Amplifier and recorded using Clampex 9, both from Molecular Devices, Sunnyvale, CA. A voltage ramp was applied to the carbon fiber. After the waveform stabilized, a pulse was applied to an adjacent region of the dorsal striatum using a stimulating electrode. The pulse was sufficient to elicit maximal stimulation, and the 2p and 4p stimuli were delivered at 100 Hz. The peak response was measured, and a single exponential fit was used to determine tau. See Perez et al., 2008; Perez et al., 2013.

Spontaneous Activity in novel environment: Mice used in the study of locomotion were eight to sixteen weeks old by the beginning of the experiment (Animal numbers: 24 lynx1WT α6L9'S, 14 lynx1KO α6L9'S, 20 lynx1WT, 18 lynx1KO). Horizontal locomotor activity was measured with an infrared photobeam activity cage system (San Diego Instruments, San Diego, CA). Ambulation events were recorded when two neighboring photobeams were broken in succession. Mice were moved to the room immediately before the experiment and put into fresh cages at the start of the novel environment test. Their activity was measured for 33 minutes. At the close of the experimental period, mice were returned to their home cages.

Automated mouse behavior analysis: Video-based software analysis of home cage behavior was conducted as described in previous literature (Steele et al., 2007; Drenan et al., 2010). Mice that were normally group housed were singly caged and habituated to the video recording room for 24 h before recording (Animal numbers: 24 lynx1WT α6L9'S, 20 lynx1KO α6L9'S, 17 lynx1WT, and 17 lynx1KO). The video recording began the following day (2 h before the dark phase) and continued for 23.5–24.0 h, using dim red lights for recording during the dark phase. The videos were analyzed using the definitions and settings described in HomeCageScan 3.0 software (Clever Sys).

Spontaneous response to nicotine injections: Acute locomotor activity in response to nicotinic ligands or other agents was studied by recording ambulation events during four 15 second intervals per minute for a designated number of minutes. This was recorded with the same equipment as the spontaneous activity assay. Groups of eight mice were singly housed in clean cages and their baseline level of activity was recorded over eight minutes (Animal numbers: 16 lynx1WT α6L9'S, 20 lynx1KO α6L9'S, 16 lynx1WT, 17 lynx1KO). Mice were removed from

their cage, injected with nicotine 0.15 mg/kg intraperitoneally (100 µl per 25 g body mass), and returned to the cage within 15 seconds. Recordings were continues for 45 minutes total.

CPP: The conditioned place preference test apparatus consists of a three chamber rectangular cage with a center neutral gray compartment (Med Associates). One test compartment is black with a stainless steel grid rod floor. The second test chamber is white with a square stainless steel mesh floor. Guillotine doors separate the chambers and can be fixed in the closed or opened position (Animal numbers: 10 lynx1WT α6L9'S, 14 lynx1KO α6L9'S, 12 lynx1WT, 16 lynx1KO).

The day before the test the animals were moved into the room with the CPP apparatus and singly housed in clean cages. The CPP protocol is a 10-day experiment in which a mouse is placed in the central compartment and allowed free access to all chambers on day one. The time spent in each chamber is recorded over a 20 minute period. Days 2-9 are training days. Intraperitoneal injections of nicotine are paired with one of the conditioning chambers, while injections of saline are paired with the other. Mice receive nicotine in the less preferred chamber as determined by day one of the experiment. The mouse receives a nicotine injection and is placed in the isolated nicotine-conditioning chamber on days 2, 4, 6, and 8. The mouse receives a saline injection and is placed in the saline chamber on days 3, 5, 7, and 9. Each training trial lasts 20 min. On the last day of the experiment, the mouse is once again given free access to all chambers for 20 min. The time spent in each chamber during baseline is subtracted from the time spent in each chamber on the final test day. A preference toward the nicotine associated chamber compared to baseline is a measure of the reward behavior associated with nicotine (Tapper et al., 2004).

Statistics: For behavioral assays we used a Kruskal-Wallis ANOVA, with post-hoc Dunn's test,

except the CPP data, which used a paired t-test. For the electrophysiology a Kruskal-Wallis ANOVA with post-hoc Dunn's test was also used. FSCV data was analyzed using a rank-sum test. Epibatidine binding used a one-way ANOVA with post-hoc comparison by Holm-Sidak test. All error bars represent the standard error of the mean.

Results

In order to test whether lynx1 interacts with α6* nicotinic receptors, we conducted a co-immunoprecpitation experiment using transfected HEK-293 cells. HEK-293 cells were transiently transfected with α6YFP or α4GFP nicotinic subunits, β2WT nicotinic subunits, and lynx1. After using an anti-GFP antibody to pull down the α6YFP fusion protein, we were able to blot for lynx1. We visualized lynx1 through an anti-lynx1 antibody (Figure 1A). When cells were transfected with either α4GFP and β2WT or α6YFP and β2WT and lynx1, we were able to visualize lynx1 on our blot. When either lynx1 or the receptor subunits were omitted or the anti-GFP antibody was not added, no lynx1 was detected (data not shown). This indicates that lynx1 binds specifically in a complex with α6YFPβ2 receptors.

Our next step was to determine if there was a functional significance to lynx1 interacting with α6* nicotinic receptors. α6* nicotinic receptors are notoriously difficult to express on the membrane in heterologous systems (Letchworth and Whiteaker, 2011). By expressing α6YFP and β2WT nAChR subunits with and without lynx1 in HEK293 cells, we tested whether expression of lynx1 would increase the expression of α6* nAChRs. The response to a puff of 300 μM nicotine was recorded using whole cell patch clamp electrophysiology. Cells were only patched if fluorescence was visualized, suggesting that α6YFP was present. In the case of α6YFPβ2WT, 12 cells were patched and puffed with nicotine. None showed a response above 10 pA. When lynx1 was transfected in addition to α6YFPβ2WT, no relative increase in response

was seen. In this case, 7 cells were puffed with nicotine and none showed a response above 10 pA. Therefore, lynx1 did not affect α6* nicotinic receptor expression in HEK293 cells.

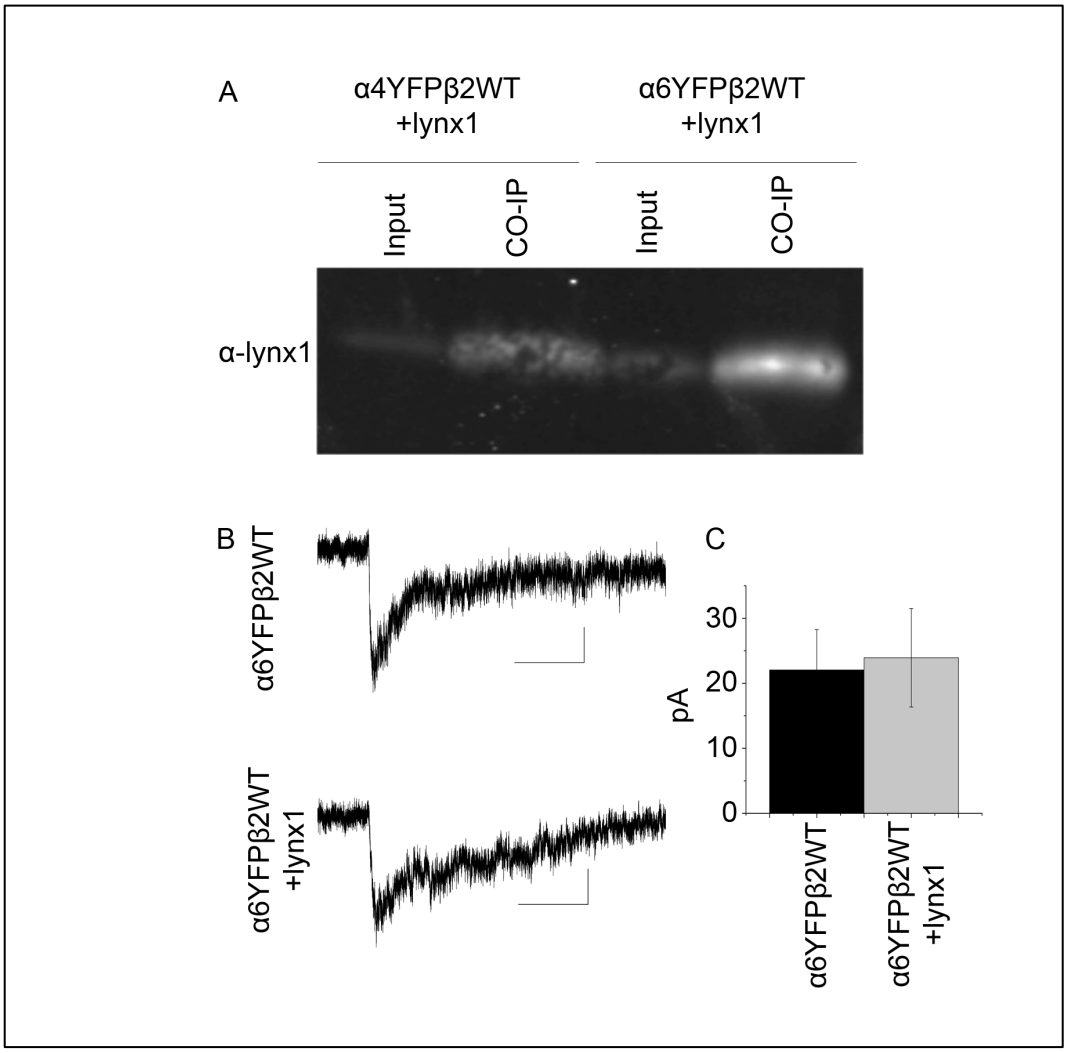

Figure 1: A) Western blot for lynx1 showing that lynx1 is pulled down when either α4GFPβ2 or α6YFPβ2 is transfected with lynx1 in HEK293 cells. B) Average traces from N2a cells transfected with either α6YFPβ2 or α6YFPβ2 + lynx1. Scale is 1 s and 5 pA for both traces. C) Graph showing average peak response to 300 μM nicotine.

Our lab has previously shown that N2a cells do express α6β2 nAChRs on the surface (Xiao et al., 2011). We tried this cell system to determine whether adding lynx1 would increase the size of the α6β2 currents recorded or the number of cells exhibiting a response. In the case of α6YFPβ2WT,

8 of 10 cells exhibited a response to 300 μM nicotine. The response size was 22.0 ± 6.2 pA. When cells were transfected with α6YFPβ2WT + lynx1, 6 of 9 cells responded. The response size was 23.9 ± 7.6 pA. Average traces are shown in Figure 1B. Adding lynx1 did not significantly affect the size of the response (Figure 1C). However, since α6* receptors are not efficiently expressed in cultured systems, this data did not confirm whether lynx1 had any effect on α6* receptors in vivo.

As mentioned in the introduction, α6* receptors are sparsely expressed in the brain. Previous studies have used mice containing hypersensitive α6* nicotinic receptors to amplify the α6* nicotinic receptor signal (Drenan et al., 2008). To study the effects of lynx1 on α6 we bred the α6L9'S mice previously generated in our lab to lynx1 KO mice (Miwa et al., 2006; Drenan et al., 2008). We hypothesized that due to the preponderance of α6* receptors expressed in the DA neurons of the α6L9'S mice, the effects of lynx1 on α6* receptors would be magnified, providing an increased probability of detecting changes in α6* nAChRs resulting from lynx1KO.

To determine whether these genetic manipulations affected the quantity of nicotinic receptors, we performed epibatidine binding in several brain regions of lynx1KO x α6L9'S mice, including striatum (ST), olfactory tubercle (OT), and superior colliculus (SC). We analyzed the sensitivity of epibatidine binding to the addition of α-CTX MII, which selectively blocks α6* receptors, to measure changes in the α6* population. Cytisine was also added to epibatidine binding to isolate the β2* nAChRs and determine if they were affected by either the addition of the L9'S mutation in the α6 nAChR subunit or knockout of lynx1. The lynx1KO mouse striatum exhibited an increase in cytisine sensitive receptors of approximately 43% ± 21% above baseline values in the wild-type mouse. The lynx1KO mice were significantly different from the lynx1KO α6L9'S mice. A comparison of the two resulted in a p-value of $p = 0.03$ (Figure 2A). However, no other

differences were detected in any of the three regions (ST, OT, or SC). The SC and OT are not shown. Though epibatidine binding does not differentiate between surface and subcellular localization of nicotinic receptors, these data indicate that generally nicotinic receptor expression is not affected by lynx1KO or α6L9'S. Previous studies evaluating epibatidine binding in α6L9'S mice have showed an increase in α-CTX MII sensitive binding in the OT and a decrease in the SC (Drenan et al., 2008). These variations were not observed in this data set. Due to the minimal change in the epibatidine binding, it was determined that the α6L9'S x lynx1KO mouse would be useful in analyzing the effect of lynx1KO on α6* receptors in the mouse brain.

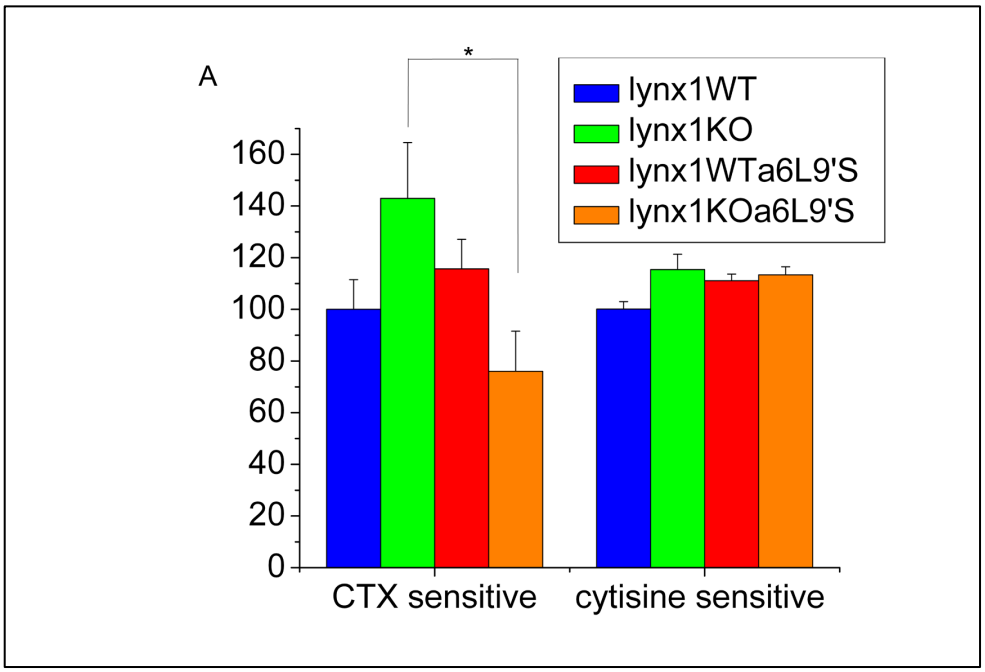

Figure 2: A) Epibatidine binding in the striatum for the four genotypes of animals used. The left side of the figure shows α-CTX MII sensitive binding; the right side shows cytisine sensitive binding.

To measure direct changes in the nicotinic receptor permeability we used $^{86}Rb+$ efflux measurements in superior colliculus synaptosomes (Figure 3, Top). We observed that lynx1KO mice had a significant decrease in the α-CTX MII sensitive $^{86}Rb+$ efflux compared to WT mice and that the α6L9'S lynx1KO mice were trending towards a decrease compared to the α6L9'S

mice (Figure 3, Top). These data suggests that there are fewer functional α6* receptors on the surface of superior colliculus cells when lynx1 is absent. The decrease in α6* receptors observed indicates that lynx1 is necessary for normal function of α6* nicotinic receptors. This could be due to a decrease in the assembly of receptors, a change in trafficking of receptors, or fewer receptors being retained on the surface.

To characterize functional changes that result from lynx1KO, striatal synaptosomes were used to measure nicotine mediated dopamine release (Figure 3, bottom). Previous studies established that the α6L9'S mice have a larger α-CTX MII component of nicotine mediated DA release, with a complimentary reduction of cytisine sensitive nicotine mediated DA release (Drenan et al., 2008). The α6L9'S nicotine mediated DA release concentration response curve is also shifted to the left, as the synaptosomes are sensitive to lower concentrations of nicotine. The lynx1WT α6L9'S mice results in this set of experiments were similar to those published previously. Notably, the α6L9'S lynx1KO mice striatal synaptosomes showed an intermediate response, with lynx1KO in the α6L9'S mice appearing to decrease the proportion of α-CTX MII sensitive receptors (Figure 3, bottom). This indicates that there is a reduction of α6* nicotinic receptor function in the absence of lynx1, but not a complete loss. The lynx1KO synaptosomes were not different from WT, which may suggest that there are not enough α6* nAChRs to detect the small changes resulting from lynx1KO modulation in the α6WT background.

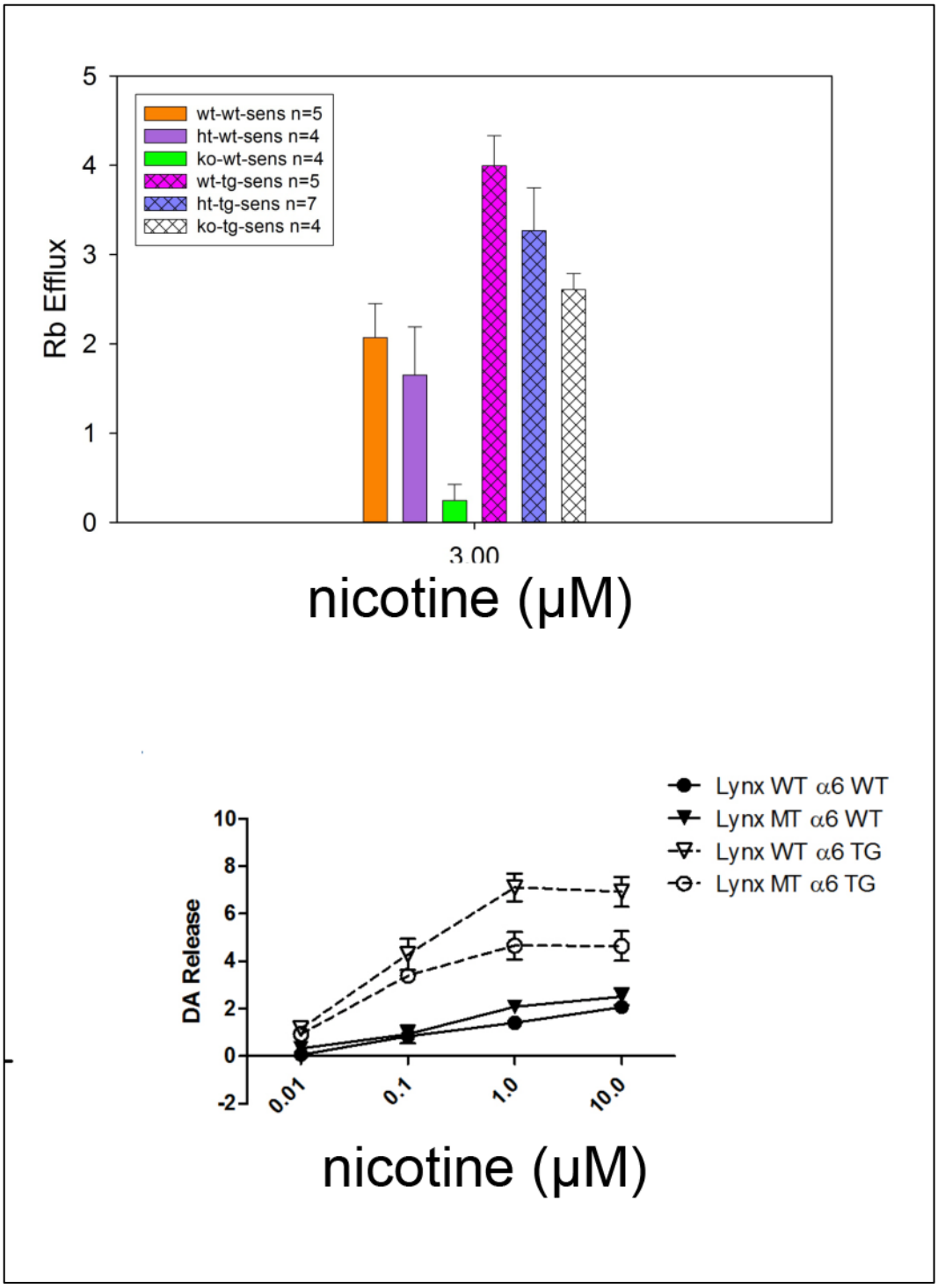

Figure 3: Top) ^{86}Rb efflux in superior colliculus synaptosomes. α-CTX MII sensitive data is shown. Bottom) Nicotine mediated dopamine release from striatal synaptosomes. α-CTX MII sensitive release is shown.

In order to directly record responses from α6* nicotinic receptors in the presence and absence of lynx1, we recorded from the SNc of lynx1KO x α6L9'S mouse brain slices. SNc DA neurons were identified, and a whole cell patch clamp configuration was obtained, followed by the application of a puff of nicotine (Figure 4A). We tested cells for I_h and for firing rate in current clamp to confirm that they were DA neurons (Drenan et al., 2008). DA cells were puffed with 1 and 10 μM nicotine, and these puffs were separated by at least 4 minutes to allow recovery from desensitization. For some cells, 100 nM α-CTX MII was perfused in the bath to block the α6 component of the nicotinic response (Figure 4B). We determined that there was no difference between WT and lynx1KO animals in the response to 1 or 10 μM nicotine (Figure 4A). However, as expected, the lynx1WT α6L9'S mouse did show an increased response to nicotine (Drenan et al., 2008). lynx1KO did not affect the size of the response to nicotine in the α6L9'S mice (Figure 4B). Adding α-CTX MII to the bath blocked the majority of the response in the lynx1WT α6L9'S and the lynx1KO α6L9'S animals, with only about 10% of the nicotine response remaining following α-CTX MII application (Figure 4C). There was no difference in the amount of signal blocked by α-CTX MII in the lynx1KO α6L9'S and the lynx1WT α6L9'S (Figure 4D). This indicates that lynx1 removal does not affect the percent of the signal contributed by α6* nicotinic receptors.

The lack of results from patch clamp recordings in the SNc was unexpected following the differences observed in the synaptosome experiments, in particular the decreased α6* component of the nicotine mediated DA release in lynx1KO α6L9'S mice compared to α6L9'S mice. We hypothesized that there may be differences at the dopaminergic terminals that are not evident at the cell body, which would explain why we did not see an effect of lynx1 in the electrophysiological experiments. This would not be surprising considering that there are known differences in the percentage of α6* receptors expressed in terminals versus the cell body (Quik et

al., 2011). Additionally, if lynx1 is acting as a chaperone for the α6* nicotinic receptors, it would be expected that removal of lynx1 would primarily affect the receptors directed to the terminals.

To resolve the observed differences between experiments done at the dopaminergic terminals versus the cell bodies, we performed fast scan cyclic voltammetry (FSCV) experiments in the dorsal striatum (Figure 4E). Previous studies have shown that the α6L9'S mouse has altered DA release in the dorsal striatum (Drenan et al., 2010; Wang et al., 2013). The α6L9'S results previously shown were confirmed in the current study. However, lynx1KO did not affect the stimulated DA release. We measured dopamine release in the lynx1KO α6L9'S mice using stimulations of 1p, 2p, 4p, and 1p following application of 100 nM α-CTX MII. Average traces and the average peak responses are shown in Figure 4C. The values for lynx1WT α6L9'S in μM DA are for 1p 0.38 ± 0.05, for 2p 0.47 ± 0.04, for 4p 0.79 ± 0.08, and for 1p + α-CTX MII 0.10 ± 0.02. The values for lynx1KO α6L9'S in μM DA are for 1p 0.53 ± 0.11, for 2p 0.76 ± 0.16, for 4p 1.05 ± 0.22, and for 1p + α-CTX MII 0.13 ± 0.04 (Figure 4F). We also compared the ratio of 4p:1p peak response (Figure 4F), and there was not a significant difference when lynx1 was knocked out. For the lynx1WT α6L9'S the ratio of 4p:1p was 2.12 ± 0.13 and for the lynx1KO α6L9'S the ratio of 4p:1p was 2.02 ± 0.13. To compare the rate of DA uptake we fit a single exponential decay to each response. We observed that there was no difference in the decay rate (tau) in the lynx1 knockout slices (data not shown). These FSCV experiments did not reveal differences between the lynx1WT α6L9'S mice and the lynx1KO α6L9'S animals in peak amplitude of response or tau.

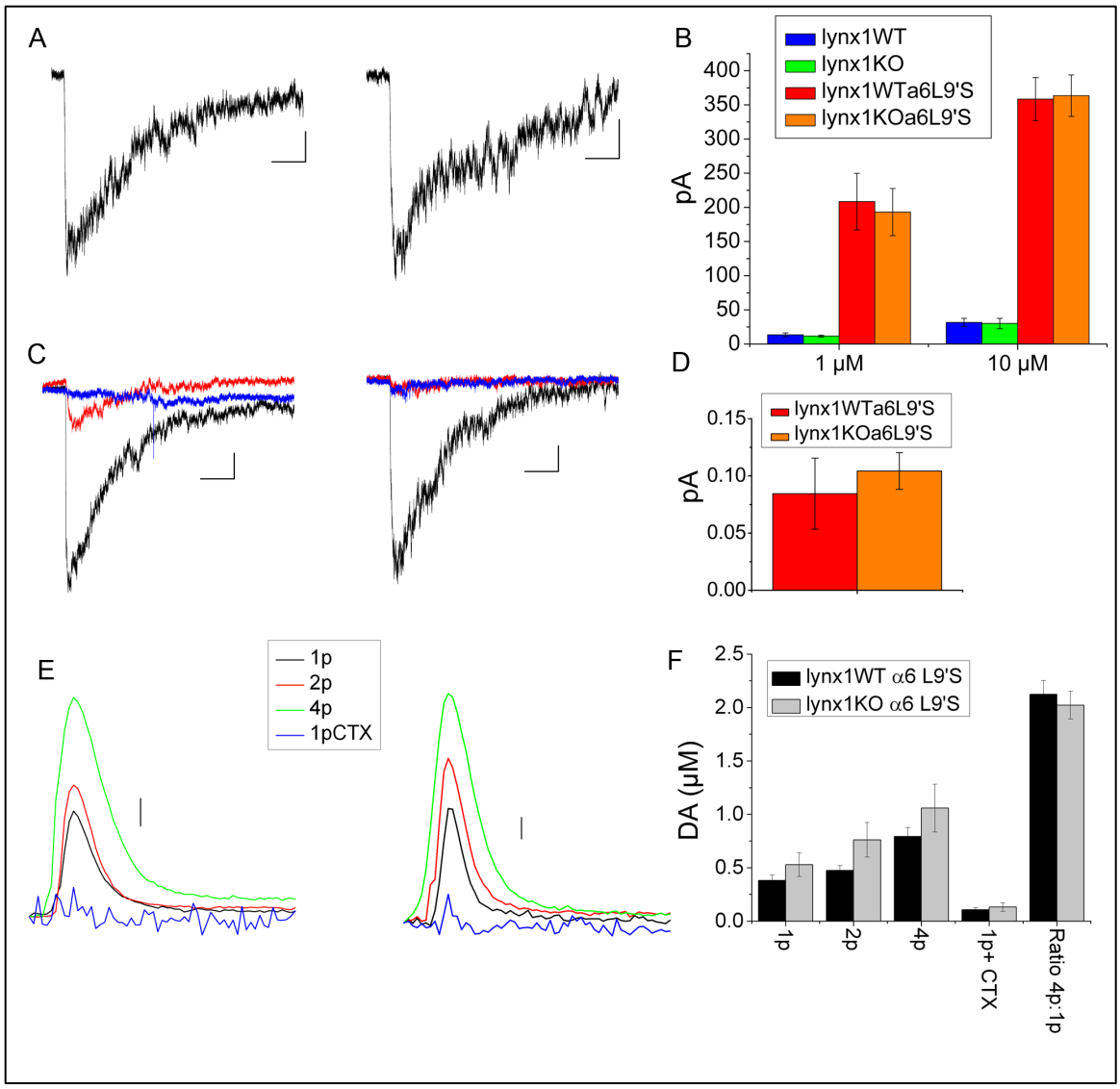

Figure 4: A) Traces from patch clamp recordings, puffed with 10 µM nicotine. Left is lynx1WT α6L9'S; right is lynx1KO α6L9'S. The scale is 2s and 50 pA. B) Average peak response to 1 and 10 µM nicotine. C) Response to 1 µM nicotine in black; red is 5 minutes after starting the flow of 100 µM α-CTX MII; blue trace is after 10 minutes of α-CTX MII. Left is lynx1WT α6L9'S; right is lynx1KO α6L9'S. The scale is 2 s and 50 pA. D) Average percentage of signal remaining after application of 100 µM α-CTX MII. E) Average DA release in response to various stimulations, as measured with FSCV. The bar represents 0.1 µM DA. F) Average peak DA response.

To see whether lynx1KO had effects on the behavioral phenotypes related to α6* nicotinic receptors we looked at the lynx1KO α69'S mice in a number of behavioral assays. The

behavioral phenotypes of the lynx1WT α6L9'S mice are striking, with some mice running over 10 km in a 24 hour period. We sought to determine whether these phenotypes were preserved in the absence of lynx1. We first tested habituation to a novel environment (Figure 5A and B). Using a ANOVA on ranks with post-hoc testing by Dunn's method, the ANOVA found a difference between the groups during minutes 12-23 ($p = 0.045$), and the Dunn's method found a difference between the lynx1WT and lynx1WT α6L9'S. During minutes 23-33, again there was a difference in the ANOVA ($p = 0.015$), but in this interval post-hoc testing found no difference. This suggests that lynx1 may have a small effect upon the expression of the phenotype. However, the variability of the α6L9'S mutation, where only a percentage of mice express the phenotype, makes it difficult to detect clear differences.

In addition to the inability to habituate, the α6L9'S mice are hyperactive during their active (dark) period. This occurs in about 35-60% of animals and depends on the exact definition of hyperactivity. We used analysis of video recordings to ascertain the distance each mouse traveled during a 24 hour home cage trial (Figure 5C). If hyperactivity is defined as movement greater than 1000 m in a 24 hour period, 14 of 24 or 58.3% of α6L9'S mice in this cohort were hyperactive. Using a more stringent cutoff of travelling 3000 m per 24 hours, 9 of 24 α6L9'S mice or 37.5% were hyperactive. As for the lynx1KO α6L9'S mice, 7 of 20 (35%) were hyperactive to the 1000 m level, while only 3 of 20 (15%) were hyperactive to the 3000 m level. However, these were not statistically significant differences. Using the Fisher's Exact Test resulted in a p-value of $p = 0.14$ with 2-tailed test for the 1000 m level and $p = 0.17$ with 2-tailed test for the 3000 m level. Comparing the four genotypes tested with an ANOVA on ranks followed by post hoc Dunn's test, we see that indeed the lynx1WT α6L9'S mice are different from WT and lynx1KO animals, but the α6L9'S lynx1KO are not significantly different from any

other genotype. It appears that there is no difference between the lynx1WT α6L9'S and the lynx1KO α6L9'S animals in hyperactive behavior.

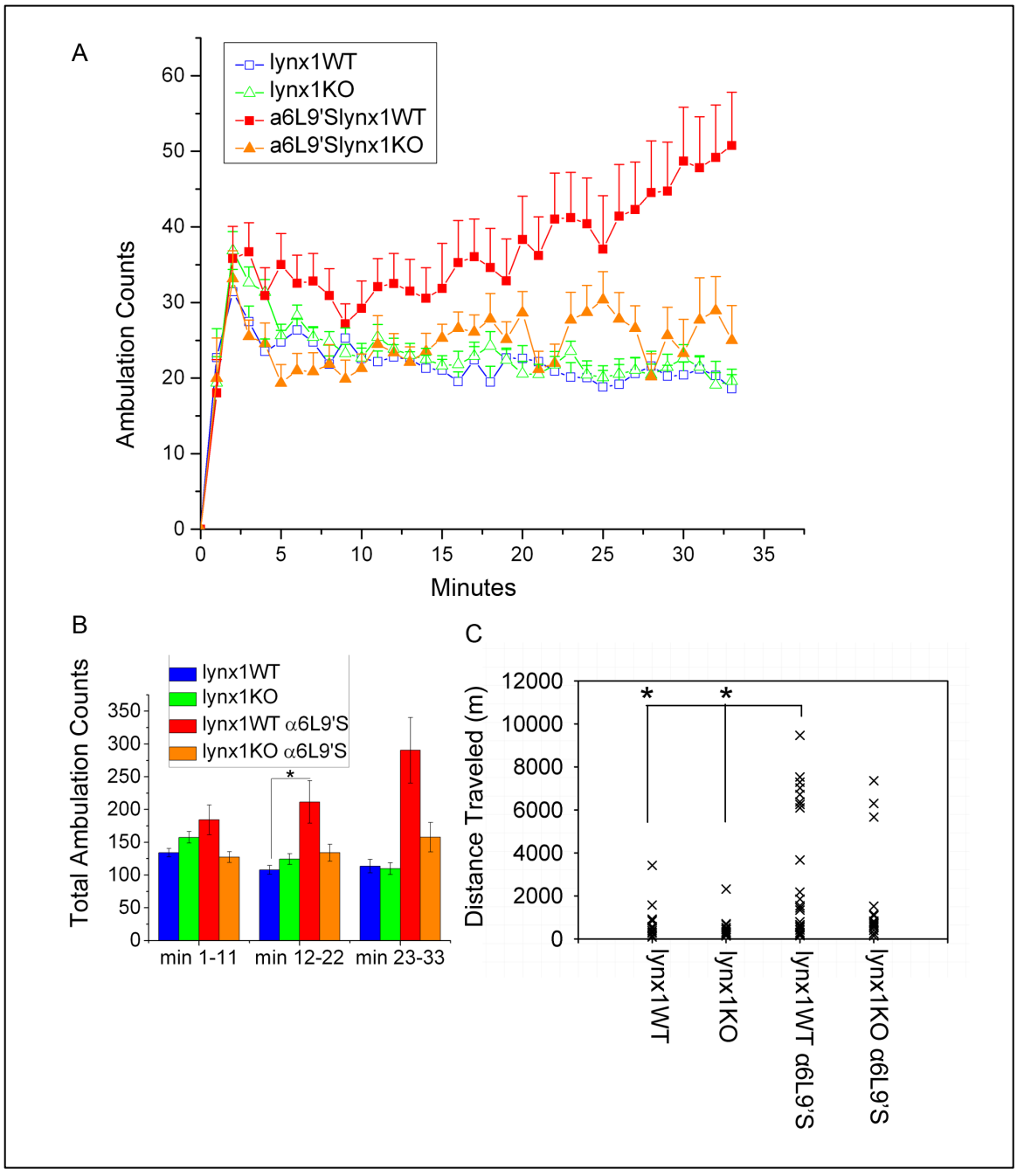

Figure 5: A) Response of mice to novel environment indicated by ambulation counts. B) Sum of ambulation counts, with the experiment split into three bins to compare the ambulation during the beginning, middle, and end of the experiment. C) Total distance traveled over 24 hours, as measured by AMBA.

Since one of the main questions of this study was to determine whether lynx1KO might have effects on α6* nicotinic receptors in the context of nicotine addiction, we also wanted to determine whether nicotine had specific effects on lynx1KO animals. Previous studies in the α6L9'S mice established that these mice are hyperactive in response to a single dose of nicotine, with the largest response occurring for an injection of 0.15 mg/kg of nicotine (free base) (Drenan et al., 2008). We injected mice with the same 0.15 mg/kg nicotine and measured their response by ambulation. The α6L9'S displayed a strong response to nicotine, reaching a peak of 58.6 ± 13.5 ambulation counts per minute (Figure 6A and B). WT mice and lynx1KO mice had peak counts of 22.4 ± 9.4 and 11.6 ± 3.1 ambulation counts per minute, respectively. lynx1KO α6L9'S mice reached peak ambulation counts of 36.9 ± 6.2 counts. Using the ANOVA on ranks produced a p-value of $p = 0.006$. Post-hoc testing revealed that lynx1WT and lynx1WT α6L9'S were significantly different from each other, but none of the other genotypes demonstrated statistically significant differences. This indicates that lynx1KO α6L9'S mice were not different from either the lynx1WT or lynx1WT α6L9'S mice.

Though we did not see an effect of nicotine on ambulation in the lynx1KO genotype, we wondered whether there would be differences in nicotine mediated reward behavior. To see whether nicotine could mediate reward in the genotypes tested, we used conditioned place preference (Figure 6C). Following previous experiments on α6L9'S, we used a nicotine dose of 0.03 mg/kg (Drenan et al., 2012). We found that the α6L9'S mice exhibited significant CPP ($p = 0.023$ with paired-test) with this dose of nicotine, as previously reported. Additionally, the lynx1KO α6L9'S mice showed significant CPP with this dose of nicotine ($p < 0.001$ with paired t-test). Neither of the genotypes (WT or lynx1KO) that did not have the α6L9'S mutation developed CPP at this dose of nicotine. These results show that there is an effect of having the

α6L9'S subunit, but no effect of lynx1KO. Therefore, it appears that lynx1 does not exhibit significant effects on nicotine-mediated reward.

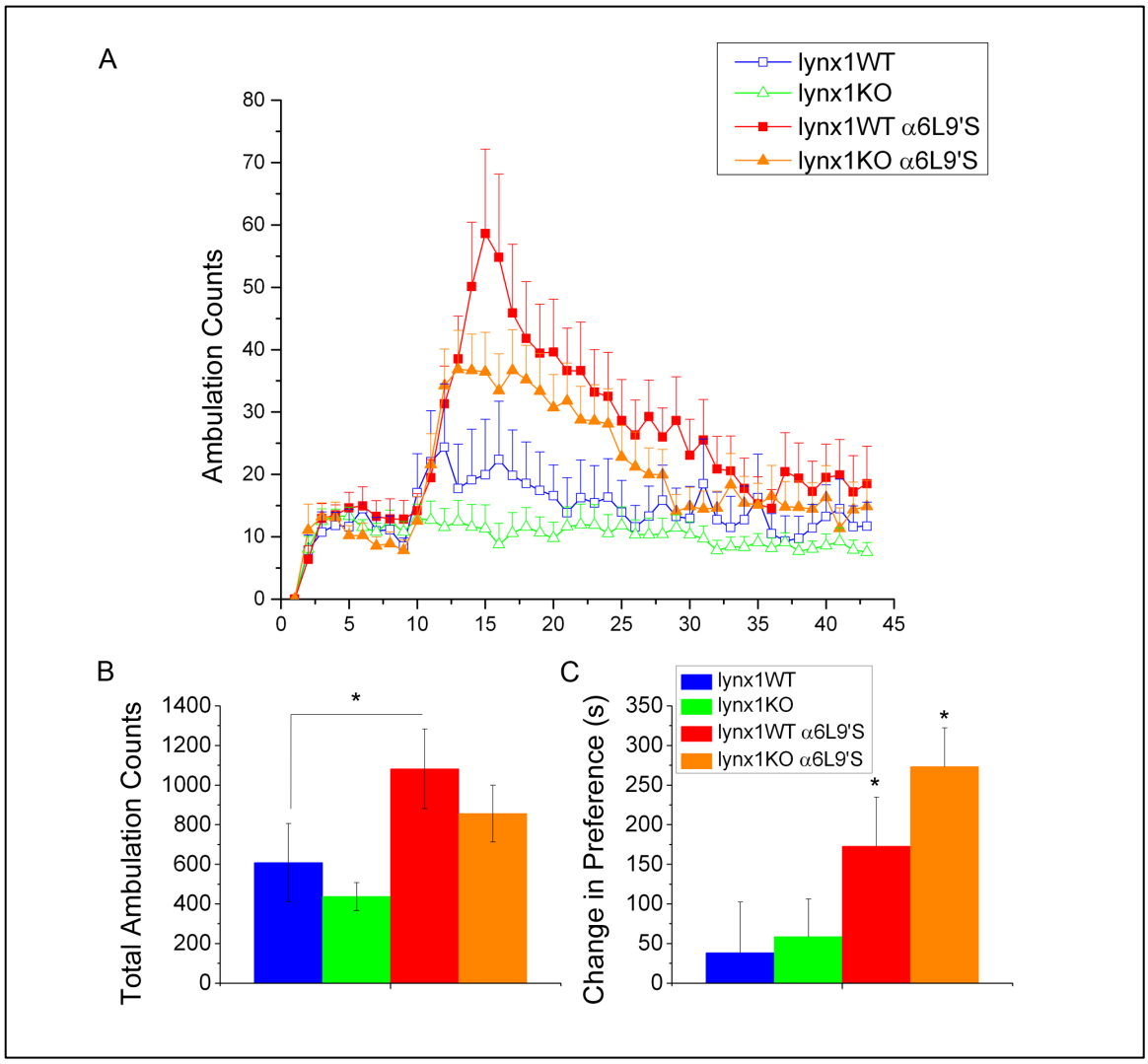

Figure 6: A) Response to a single injection of 0.15 mg/kg of nicotine. B) Averaged sum of ambulation counts during single injection experiment. C) Average change in preference for mice undergoing CPP protocol with dose of 0.03 mg/kg of nicotine. Each training and testing session was 20 minutes long.

Discussion:

lynx1 does affect α6* nicotinic receptors. However, these effects appear to be in certain brain regions and in very specific circumstances. lynx1 can associate with α6YFPβ2 when transiently

overexpressed in cell lines, but the addition of lynx1 did not affect the response to nicotine in transfected cells. It may be that cell lines are not an appropriate expression system for the α6* nicotinic receptor and that functional differences must be studied in neurons. We used the lynx1KO and α6L9'S mouse models to study the effects of lynx1 on α6 in vivo. Since these receptors are normally present in specific brain regions, we looked to see whether those brain regions exhibited any changes when lynx1 was knocked out.

Using synaptosomes prepared from mice, we discerned that lynx1KO reduced the amount of ^{86}Rb+ efflux in the superior colliculus, suggesting that there were fewer functional nicotinic receptors when lynx1 was absent. This data indicates that lynx1 is necessary for the normal function of α6* nicotinic receptors. Additional data to support this hypothesis comes from the nicotine mediated DA release experiments, which showed that lynx1KO reduced α-CTX MII sensitive DA release in α6L9'S mice. However, neither patch clamp electrophysiology of DA neurons in the SNc nor voltammetry in the striatum detected any effect of lynx1KO. Behavioral assays demonstrated a trend towards decreased habituation and decreased spontaneous activity, but these were not statistically significant. The behavioral data suggest that there may be an effect of lynx1KO, but the high amount of variability in the lynx1WT α6L9'S mice make it difficult to isolate the effects of lynx1 knockout.

The synaptosome experiments provide evidence of the necessity of lynx1 for the normal function of α6* nicotinic receptors. However, we were not able to recapitulate these findings with electrophysiology or FSCV in brain slices. First, in slice electrophysiology of the SNc, we did not see an effect of lynx1KO. There are several possible explanations for this apparent inconsistency. lynx1 may have differential effects on nicotinic receptors that are localized on the cell body versus the terminals of these neurons. Additionally, lynx1 may be necessary for normal targeting

of the α6* receptors to the DA terminals, causing differences in the terminals that are undetectable when recordings are done from the cell bodies.

To try to address the possibility of variation between the terminals and cell bodies, we used FSCV in the dorsal striatum to measure DA release. In agreement with previously published data, we saw significant increase in the size of the response from 1p to 4p. The addition of α-CTX MII reduced DA release by approximately 90%, far greater than what has previously been seen in WT mice, but consistent with previous reports in the α6L9'S mice (Wang et al., 2013). However, we did not measure any differences in lynx1KO α6L9'S mice and α6L9'S mice in the presence of α-CTX MII. This was surprising given the differences seen in the nicotine mediated DA release, which did note differences in the presence of α-CTX MII. However, these are very different assays. The FSCV experiments use electrical stimulation, and in our case we used a maximal stimulation with 100 Hz. More subtle differences in electrically stimulated DA release may be seen if a range of stimulation strengths and frequencies are used. Additionally, application of optogenentics could provide a better picture of whether lynx1 is affecting α6* mediated DA release. Studies into the mechanism of DA release have shown that coordinated activation of cholinergic interneurons in the striatum is sufficient to cause nicotinic mediated DA release (Cachope et al., 2012; Threlfell et al., 2012). Applying this method of stimulation might provide a means to determine the effects of lynx1 in ways that cannot be revealed by electrical stimulation of the striatum.

Previous studies have shown that lynx1 acts as a brake or a negative modulator of nicotinic receptors. However, this was not the case with α6* nicotinic receptors. The effects of lynx1 on α6* nicotinic receptors appears to be paradoxical to its effects on α4β2 and α7 nicotinic receptors (Miwa et al., 1999; Ibanez-Tallon et al., 2002; Miwa et al., 2006). The data in this paper

demonstrate that lynx1KO normally augments the function of α6* nicotinic receptors, and that removing lynx1 actually dampens their activity. This was unexpected and indicates that the α6 nicotinic receptor subunit likely has a specialized interaction with lynx1. Another unanticipated finding was the lack of effect of lynx1 on non-α6* nicotinic receptors in the brain regions currently under investigation. Based on previous knowledge of lynx1, lynx1KO would be expected to have effects in the α-CTX MII resistant populations of nicotinic receptors in the dopaminergic neurons, which include α4β2 and α5α4β2 (Champtiaux et al., 2003; Grady et al., 2007). We did not see any effects on α-CTX MII resistant populations, in synaptosomes, electrophysiology, or FSCV experiments. It could be that the effects of lynx1 are specific to different brain regions. Another possibility is that other modulators of nicotinic receptors are present in dopaminergic neurons, and their effects negate or considerably dampen the effects of lynx1 knockout. There are several members of the lynx1 family expressed in the brain. There may be other family members present in dopaminergic neurons which are able to function in the absence of lynx1 to keep the brake on α4β2 nicotinic receptors (Miwa et al., 2012).

In summary, we have found that α6* nicotinic receptors are modulated by lynx1. This represents a new method of regulation for this subclass of nicotinic receptors. While we did not find any connection between lynx1KO and addiction, there may be other similar mechanisms of modulation of α6* nicotinic receptors that would be helpful in combating addiction.

Acknowledgements:

Thank you to J. Michael McIntosh for providing α-CTX MII.

References:

Brunzell DH (2012) Preclinical Evidence That Activation of Mesolimbic Alpha 6 Subunit Containing Nicotinic Acetylcholine Rceptors Supports Nicotine Addiction Phenotype. Nicotine & Tobacco Research : official journal of the Society for Research on Nicotine and Tobacco 14:1258-1269.

Cachope R, Mateo Y, Mathur BN, Irving J, Wang H-L, Morales M, Lovinger DM, Cheer JF (2012) Selective activation of cholinergic interneurons enhances accumbal phasic dopamine release: setting the tone for reward processing. Cell Reports 2:33-41.

Champtiaux N, Gotti C, Cordero-Erausquin M, David DJ, Przybylski C, Lena C, Clementi F, Moretti M, Rossi FM, Le Novere N, McIntosh JM, Gardier AM, Changeux JP (2003) Subunit composition of functional nicotinic receptors in dopaminergic neurons investigated with knock-out mice. J Neurosci 23:7820-7829.

Drenan RM, Lester HA (2012) Insights into the Neurobiology of the Nicotinic Cholinergic System and Nicotine Addiction from Mice Expressing Nicotinic Receptors Harboring Gain-of-Function Mutations. Pharmacological reviews.

Drenan RM, Engle S, Lester HA, McIntosh JM, Brunzell DH (2012) Activation of α6β2* nicotinic acetylcholine receptors is sufficient for nicotine reward. In: Society for Neuroscience. New Orleans, LA: Program No. 455.03 Neuroscience Meeting Planner.

Drenan RM, Grady SR, Steele AD, McKinney S, Patzlaff NE, McIntosh JM, Marks MJ, Miwa JM, Lester HA (2010) Cholinergic modulation of locomotion and striatal dopamine release is mediated by α6α4* nicotinic acetylcholine receptors. J Neurosci 30:9877-9889.

Drenan RM, Grady SR, Whiteaker P, McClure-Begley T, McKinney SR, Miwa J, Bupp S, Heintz N, McIntosh JM, Bencherif M, Marks MA, Lester HA (2008) *In Vivo* Activation of Midbrain Dopamine Neurons via Sensitized, High-Affinity α6* Nicotinic Acetylcholine Receptors. Neuron 60:123-136.

Exley R, Clements MA, Hartung H, McIntosh JM, Cragg SJ (2008) α6-Containing Nicotinic Acetylcholine Receptors Dominate the Nicotine Control of Dopamine Neurotransmission in Nucleus Accumbens. Neuropsychopharmacology 33:2158-2166.

Grady SR, Salminen O, Laverty DC, Whiteaker P, McIntosh JM, Collins AC, Marks MJ (2007) The subtypes of nicotinic acetylcholine receptors on dopaminergic terminals of mouse striatum. Biochem Pharmacol 74:1235-1246.

Ibanez-Tallon I, Miwa JM, Wang HL, Adams NC, Crabtree GW, Sine SM, Heintz N (2002) Novel modulation of neuronal nicotinic acetylcholine receptors by association with the endogenous prototoxin lynx1. Neuron 33:893-903.

Jackson KJ, McIntosh JM, Brunzell DH, Sanjakdar SS, Damaj MI (2009) The Role of α6-Containing Nicotinic Acetylcholine Receptors in Nicotine Reward and Withdrawal. The Journal of pharmacology and experimental therapeutics 331:547-554.

Letchworth SR, Whiteaker P (2011) Progress and challenges in the study of α6-containing nicotinic acetylcholine receptors. Biochemical pharmacology 82:862-872.

Mackey ED, Engle SE, Kim MR, O'Neill HC, Wageman CR, Patzlaff NE, Wang Y, Grady SR, McIntosh JM, Marks MJ, Lester HA, Drenan RM (2012) α6* Nicotinic Acetylcholine Receptor Expression and Function in a Visual Salience Circuit. J neurosci 32:10226-10237.

Miwa JM, Lester HA, Walz A (2012) Optimizing cholinergic tone through lynx modulators of nicotinic receptors: implications for plasticity and nicotine addiction. Physiology 27:187-199.

Miwa JM, Ibanez-Tallon I, Crabtree GW, Sanchez R, Sali A, Role LW, Heintz N (1999) lynx1, an endogenous toxin-like modulator of nicotinic acetylcholine receptors in the mammalian CNS. Neuron 23:105-114.

Miwa JM, Stevens TR, King SL, Caldarone BJ, Ibanez-Tallon I, Xiao C, Fitzsimonds RM, Pavlides C, Lester HA, Picciotto MR, Heintz N (2006) The Prototoxin lynx1 Acts on Nicotinic Acetylcholine Receptors to Balance Neuronal Activity and Survival In Vivo. Neuron 51:587-600.

Morishita H, Miwa J, Heintz N, Hensch T (2010) Lynx1, a cholinergic brake, limits plasticity in adult visual cortex. Science 330:1238-1240.

Nashmi R, Xiao C, Deshpande P, McKinney S, Grady SR, Whiteaker P, Huang Q, McClure-Begley T, Lindstrom JM, Labarca C, Collins AC, Marks MJ, Lester HA (2007) Chronic nicotine cell specifically upregulates functional α4* nicotinic receptors: basis for both tolerance in midbrain and enhanced long-term potentiation in perforant path. J Neurosci 27:8202-8218.

Perez XA, McIntosh JM, Quik M (2013) Long-term nicotine treatment down-regulates α6β2* nicotinic receptor expression and function in nucleus accumbens. Journal of Neurochemistry 127:762-771.

Perez XA, Parameswaran N, Huang LZ, O'Leary KT, Quik M (2008) Pre-synaptic dopaminergic compensation after moderate nigrostriatal damage in non-human primates. Journal of Neurochemistry 105:1861-1872.

Pons S, Fattore L, Cossu G, Tolu S, Porcu E, McIntosh JM, Changeux JP, Maskos U, Fratta W (2008) Crucial role of α4 and α6 nicotinic acetylcholine receptor subunits from ventral tegmental area in systemic nicotine self-administration. J Neurosci 28:12318-12327.

Powers MS, Broderick HJ, Drenan RM, Chester JA (2013) Nicotinic acetylcholine receptors containing α6 subunits contribute to alcohol reward-related behaviours. Genes, brain, and behavior:n/a-n/a.

Quik M, Perez XA, Grady SR (2011) Role of α6 nicotinic receptors in CNS dopaminergic function: Relevance to addiction and neurological disorders. Biochem Pharmacol.

Steele AD, Jackson WS, King OD, Lindquist S (2007) The power of automated high-resolution behavior analysis revealed by its application to mouse models of Huntington's and prion diseases. Proceedings Of The National Academy Of Sciences Of The United States Of America 104:1983-1988.

Tapper AR, McKinney SL, Nashmi R, Schwarz J, Deshpande P, Labarca C, Whiteaker P, Marks MJ, Collins AC, Lester HA (2004) Nicotine activation of α4* receptors: sufficient for reward, tolerance and sensitization. Science 306:1029-1032.

Threlfell S, Lalic T, Platt NJ, Jennings KA, Deisseroth K, Cragg SJ (2012) Striatal dopamine release is triggered by synchronized activity in cholinergic interneurons. Neuron 75:58-64.

Wang Y, Lee J-W, Oh G, Grady SR, McIntosh JM, Brunzell DH, Cannon JR, Drenan RM (2013) Enhanced synthesis and release of dopamine in transgenic mice with gain-of-function α6* nAChRs. Journal of Neurochemistry 129:315-327.

Whiteaker P, McIntosh JM, Luo S, Collins AC, Marks MJ (2000) ^{125}I-α-conotoxin MII identifies a novel nicotinic acetylcholine receptor population in mouse brain. Molecular Pharmacology 57:913-925.

Xiao C, Srinivasan R, Drenan RM, Mackey ED, McIntosh JM, Lester HA (2011) Characterizing functional α6β2 nicotinic acetylcholine receptors in vitro: mutant β2 subunits improve membrane expression, and fluorescent proteins reveal responsive cells. Biochem Pharmacol 82:852-861.

Chapter 2

Additional data for lynx1 modulation of α6 nicotinic receptors

This chapter will present data related to the effect of lynx1 on α6* nicotinic receptors discussed in the previous chapter. Necessarily, the previous chapter does not include all of the data that was collected for this project. This chapter will provide additional figures and analysis of the interaction between lynx1 and α6* related to the previous chapter.

Based on the data presented in Chapter 1, we concluded that lynx1 does have minor effects on α6* nicotinic receptors. Two separate synaptosomal experiments showed statistically significant effects of lynx1 on α6* receptors. ^{86}Rubidium Efflux from superior colliculus synaptosomes indicated that lynx1KO reduced the amount of functional α6* receptors. In addition, we saw that nicotine mediated DA release is reduced in the lynx1KO α6L9'S mice compared to the lynx1WT α6L9'S using striatal synaptosomes.

The statistically significant results in synaptosomal experiments indicated that pursuing the study of the effects of lynx1 on α6* nicotinic receptors could prove fruitful. I undertook a number of experiments, utilizing a variety of experimental techniques, including electrophysiology, voltammetry, and behavior, in order to more fully understand the interaction between lynx1 and α6* nicotinic receptors. As noted in the previous chapter, it proved difficult to isolate the effects of lynx1 and build upon the above results. In attempting to find statistically significant effects of lynx1 on α6* nicotinic receptors, I did extensive analysis of the various types of data produced

within this project. This chapter presents that analysis and more clearly demonstrates the reasoning behind the different experimental methods.

As indicated in the previous chapter, I conducted a CO-IP experiment to determine whether lynx1 could bind α6* nicotinic receptors. CO-IP experiments can be difficult to interpret, so the data presented here shows some of the additional controls that were used. Using HEK293 cells, which express large amounts of protein, we were able to pull down α4GFPβ2 and α6YFPβ2 nicotinic receptors using an anti-GFP antibody. We then performed a western blot for lynx1. Using an anti-lynx1 antibody, we were able to detect the presence of lynx1. Several negative controls were done, including leaving out the anti-GFP antibody, leaving out lynx1, and leaving out the nicotinic receptors (Figure 2.1). The negative controls show that there is an interaction between lynx1 and α6YFPβ2. We do not know if this interaction is something that occurs in neurons in vivo. One possibility is that the transient overexpression has caused an interaction that would not normally be present in neurons. We conclude that it is likely that lynx1 does bind α6* nicotinic receptors, but we do not have direct confirmation from neurons that normally express these proteins.

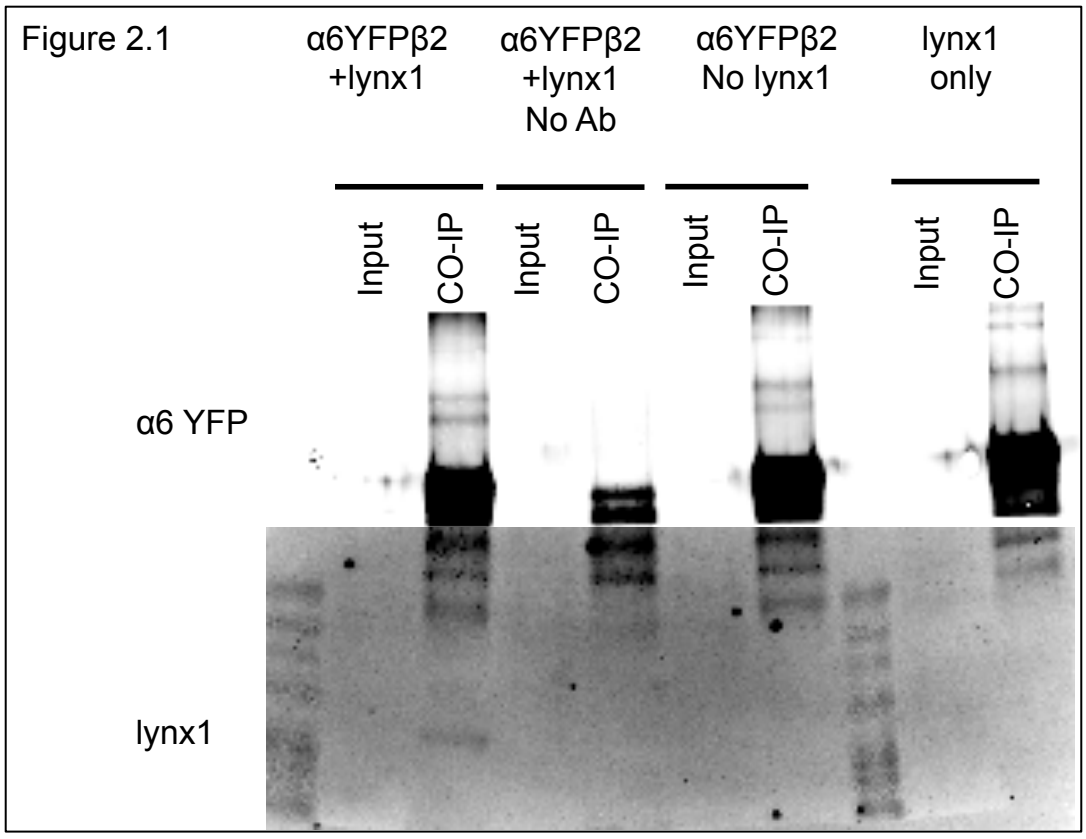

Figure 2.1: CO-Immunoprecipitation of α6YFPβ2 nicotinic receptors and lynx1.

Patch clamp electrophysiology and fast scan cyclic voltammetry techniques were used to look for functional differences in the lynx1KO mice. We did not see any effects of lynx1KO on α6* nicotinic receptors. In Chapter 1, patch clamp electrophysiology recordings from the SNc were presented. Traces of nicotinic puffs and averaged peak response were shown in Figure 1.4A and B. These recordings are done in slices, so there is a risk of recording from other cell types, such as GABAergic neurons. To ensure that recordings were from dopaminergic neurons and not other cell types, two electrophysiological controls were used in each cell. Testing was done for I_h, the hyperpolarization activated current, which is seen as a sag in current when a cell is hyperpolarized (Figure 2.2A). Additionally, each cell was switched to current clamp mode to observe the natural firing rate of the cell, and cells that were firing above the normal tonic firing

rate of DA neurons (1-4 Hz) were discarded (Figure 2.2B). A picture of the patch electrode placement for each cell was taken, which confirmed that the recording was from an appropriate region (Figure 2.3).

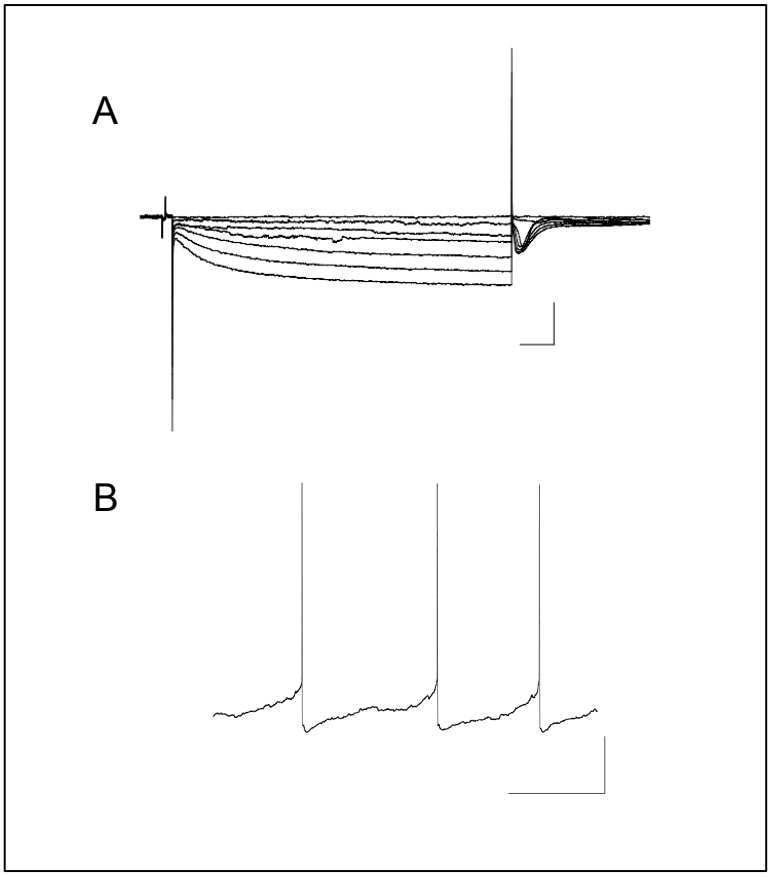

Figure 2.2: A) Patch clamp recording from putative dopaminergic neuron, showing I_h. Scale is 200 ms and 500 pA. B) Current clamp recording showing firing of DA neuron scale is 500 ms and 20 mV.

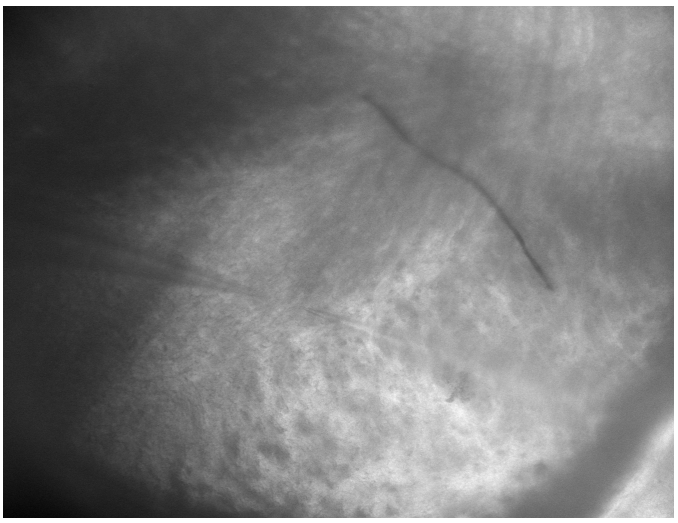

Figure 2.3: Picture taken during recording using 10x objective. Patch pipette is on the right and nicotine puffer pipette is on the left. The edge of the slice is seen in the lower right corner of the image.

In addition to the nicotine mediated response of DA neurons, we determined whether there were changes in the absence of nicotine activation. We measured the tonic firing rate of DA neurons in SNc neurons. Nicotine can affect the tonic firing rate of DA neurons, so it is possible that lynx1KO, by affecting nicotinic receptors, may have an effect as well. Acute nicotine increases the firing rate of DA neurons in freely moving rats (Zhang et al., 2009). Chronic nicotine also decreases the firing rate of SNc DA neurons in WT but not α4KO animals (Xiao et al., 2009). To determine whether lynx1KO had similar effects, we took one minute recordings in current clamp mode and measured the average firing rate (Figure 2.4). The values for lynx1WT were 1.70 ± 0.15; lynx1KO 1.47 ± 0.30; lynx1WT α6L9'S 1.30 ± 0.17; and lynx1KO α6L9'S ± 0.14. A one-way ANOVA did not detect a significant difference between the groups. Perhaps chronic treatment with nicotine in the lynx1KO animals would amplify differences that we did not see in this study.

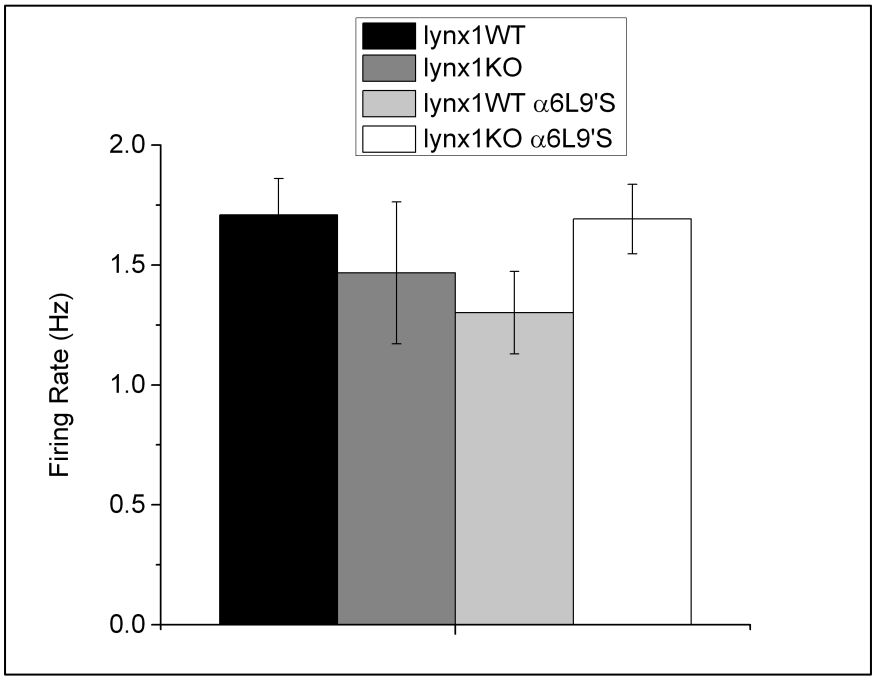

Figure 2.4: Average firing rate of DA neurons in current clamp. Data are from 14 lynx1WT cells, 12 lynx1KO cells, 21 lynx1WT α6L9'S, and 22 lynx1KO α6L9'S cells.

Electrophysiology traces can reveal much more than peak response: they can reveal what the electrophysiologist that collected them ate for breakfast. Therefore, I have analyzed the decay time, rise time, and net charge in response to a puff of nicotine in the SNc. The peak response to nicotine was already presented in Chapter 1, Figure 1.4A and B. Both rise time and decay time are the values taken between 10% to 90% of the peak response (Figure 2.5, 2.6). Net charge is measured by taking the area under the curve (Figure 2.7). As with the peak response, there was no difference when lynx1 was knocked out. This conflicted with the data taken from the synaptosomes, which saw a decrease in α6 mediated effects when lynx1 was knocked out.

The most obvious difference between the synaptosomal data and the patch clamp recordings was the location from which the data was collected. The synaptosomes were taken from several different sites, but the differences in the nicotine mediated DA release were seen in the striatum,

which is where the terminals of the SNc DA neurons are located. The SNc cell bodies were the location of the patch clamp recordings. It is known that there are differences in the types of nicotinic receptors located on the terminals and the cell bodies (Champtiaux et al., 2003). Champtiaux et al. showed that about 20% of α4β2* receptors at the cell bodies contain α6, while at the terminals there is approximately a 50:50 split between α4β2 nicotinic receptors with and without α6. This difference in α6* nicotinic receptor ratio may explain why we were able to detect an effect of lynx1 from synaptosomes when we did not see effects in patch clamp recordings. We also have not been able to answer whether the function of lynx1 itself is compartmentalized, with different effects at cell bodies versus synaptic terminals.

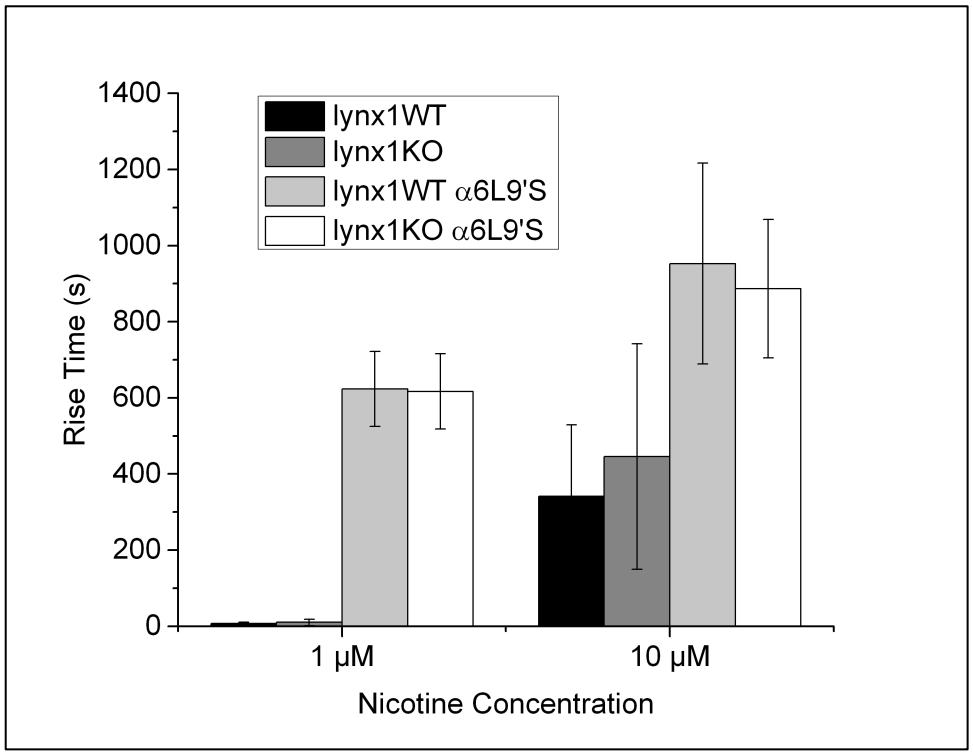

Figure 2.5: 10%-90% rise time of response to either 1 μM or 10 μM of nicotine. 1 μM data are from 7 lynx1WT cells, 5 lynx1KO cells, 11 lynx1WT α6L9'S, and 15 lynx1KO α6L9'S cells. 10 μM data are from 7 lynx1WT cells, 5 lynx1KO cells, 12 lynx1WT α6L9'S, and 17 lynx1KO α6L9'S cells.

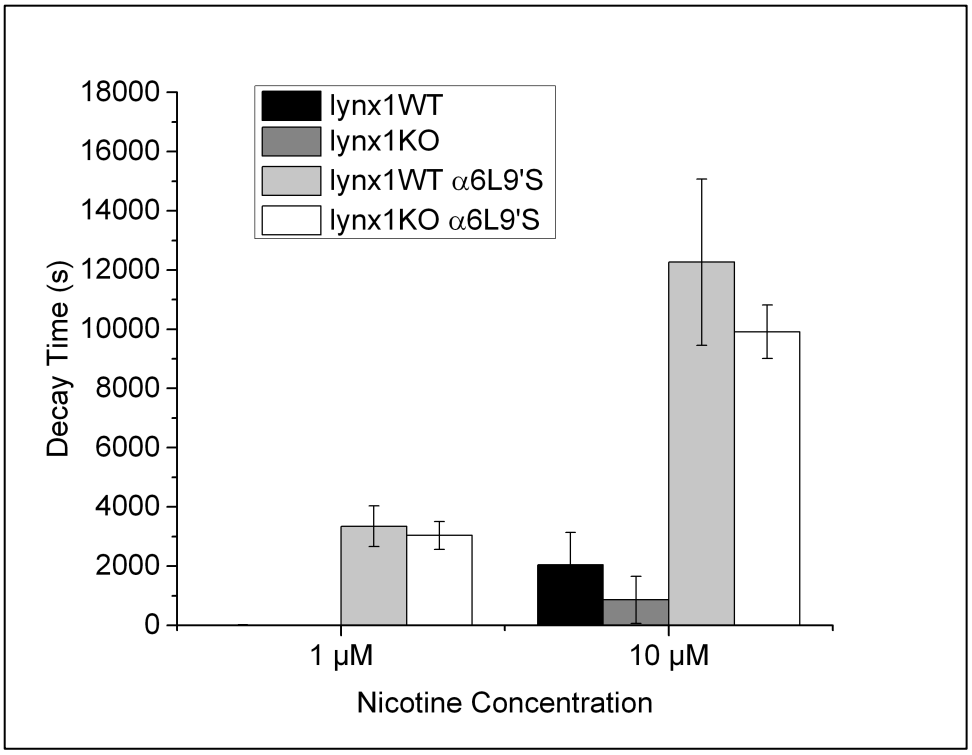

Figure 2.6: 10%-90% decay time of response to either 1 μM or 10 μM of nicotine. Number of cells is the same as for Figure 2.5

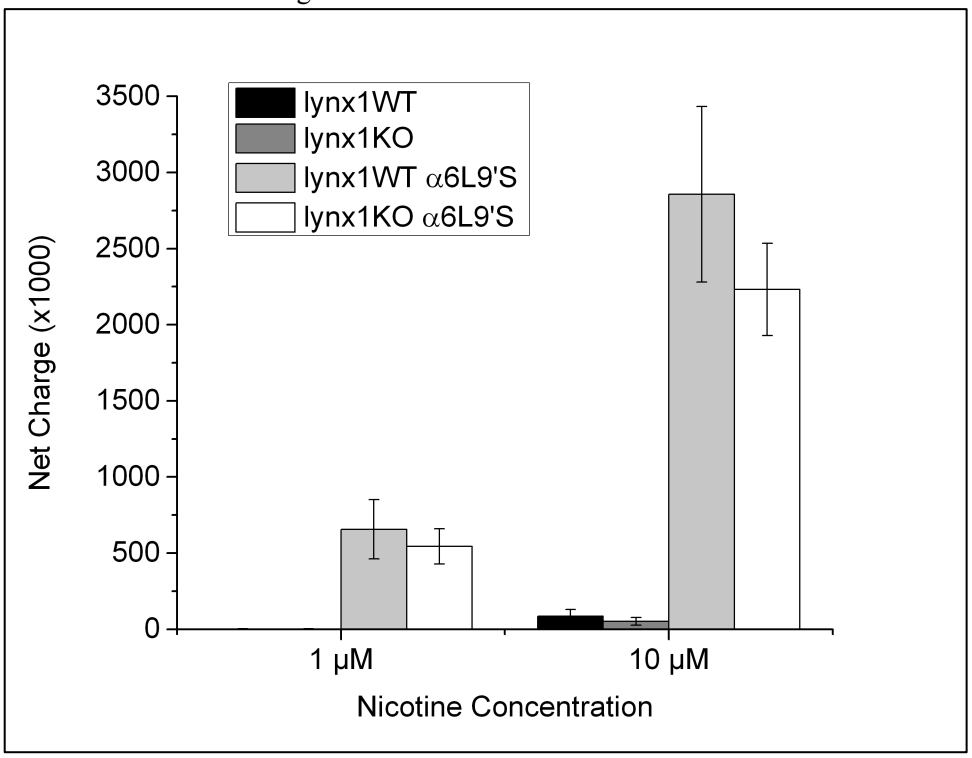

Figure 2.7: Total Area under the curve (net charge) of responses to either 1 μM or 10 μM of nicotine. Number of cells is the same as for Figure 2.5

The way that we approached the conflict between the synaptosome and patch physiology data was to try to confirm the effect of lynx1 at the terminals. We measured DA release via FSCV. FSCV can be used to determine the amount of dopamine release in response to a stimulating electrode that is placed nearby. By applying a voltage to the carbon fiber electrode a cyclic voltamogram is produced, which can be used to identify neurotransmitters such as dopamine (Robinson et al., 2003). In wild type slices from the dorsal striatum, the response to a single pulse or to a train of pulses is the same size. This is due to synaptic depression (Cragg, 2003). The addition of nicotine relieves that depression so that a 2p or 4p stimulation is larger than a 1p stimulation (Rice and Cragg, 2004). Rice and Cragg also showed that nicotine causes the response to a single pulse to be decreased compared to an untreated slice. Previous studies have shown that the α6L9'S mice also lack depression during multiple pulses, and that as the number of pulses increases the size of the response increases (Drenan et al., 2010; Wang et al., 2013). We found that lynx1KO did not affect DA release in α6L9'S mice (Figure 1.4E and F). The previous study by Drenan et al. noted that the tau of the response was increased in the α6L9'S mice. We confirmed that result in the lynx1WT α6L9'S mice and found that tau was unaffected by lynx1KO (Figure 2.8). Finally, we have limited data of a 4p stimulus after α-CTX MII, which suggests that lynx1KO effects are not overcome with the stronger stimulus in the presence of α-CTX MII (Figure 2.9).

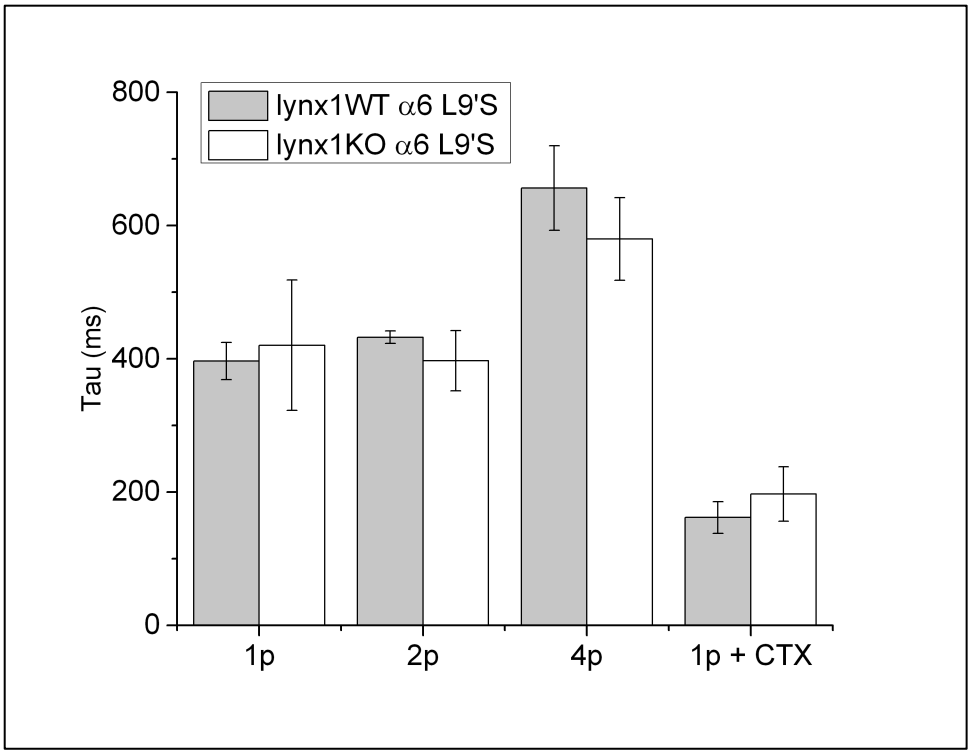

Figure 2.8: Average Tau measured after fitting the DA response to a single exponential decay.

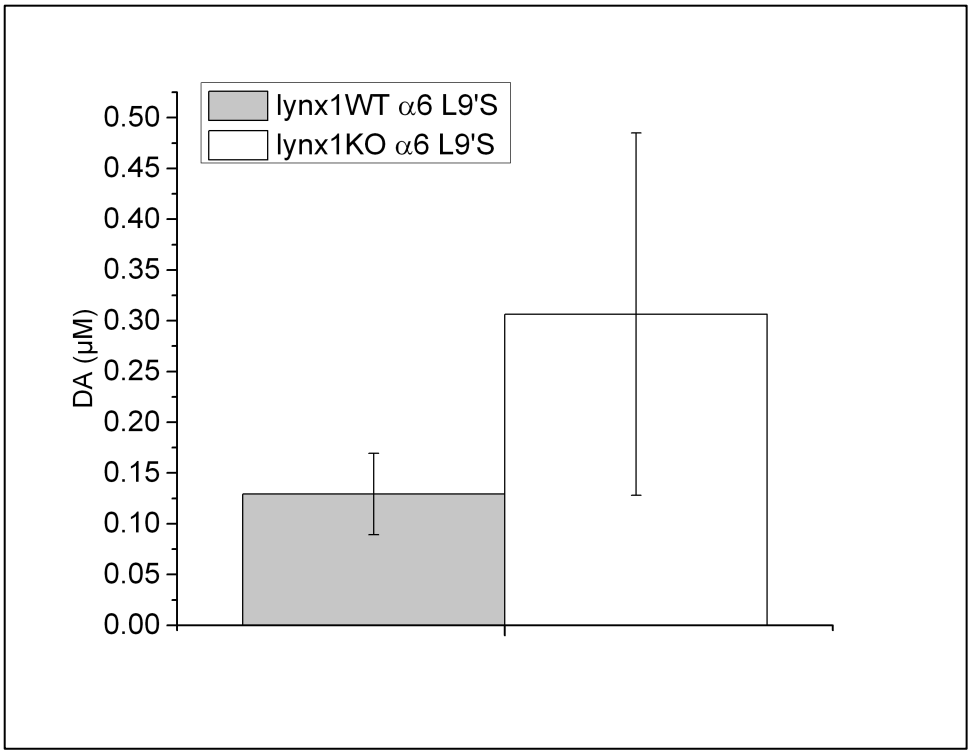

Figure 2.9: Average DA release following treatment with 100 μM αCTX-MII, with 4p 100 Hz stimulus (2 lynx1WT α6L9'S locations and 3 lynx1KO α6L9'S locations).

This chapter has presented some additional information and analysis regarding the effect of lynx1KO on α6 nicotinic receptors. Unfortunately, we did not discover any additional effects of lynx1KO. We considered several reasons as to why that might be the case, which were addressed in the discussion of Chapter 1. To recap, we saw an effect of lynx1KO in striatal synaptosomes but not in striatal FSCV recordings. It could be that the electrical stimulation of FSCV was too general compared to nicotine mediated release in the synaptosomes. The electrical stimulation stimulates all axons in the vicinity, which might wash out effects of lynx1. Also, we used a maximal stimulation at 100 Hz for FSCV, perhaps a submaximal stimulation would be better at revealing differences between lynx1KO and lynx1WT. Any future studies would have to consider this and should also consider using optogenetics to specifically target different subclasses of striatal neuron populations.

References

Champtiaux N, Gotti C, Cordero-Erausquin M, David DJ, Przybylski C, Lena C, Clementi F, Moretti M, Rossi FM, Le Novere N, McIntosh JM, Gardier AM, Changeux JP (2003) Subunit composition of functional nicotinic receptors in dopaminergic neurons investigated with knock-out mice. J Neurosci 23:7820-7829.

Cragg SJ (2003) Variable dopamine release probability and short-term plasticity between functional domains of the primate striatum. J Neurosci 23:4378-4385.

Drenan RM, Grady SR, Steele AD, McKinney S, Patzlaff NE, McIntosh JM, Marks MJ, Miwa JM, Lester HA (2010) Cholinergic modulation of locomotion and striatal dopamine release is mediated by α6α4* nicotinic acetylcholine receptors. J Neurosci 30:9877-9889.

Rice ME, Cragg SJ (2004) Nicotine amplifies reward-related dopamine signals in striatum. Nat Neurosci 7:583-584.

Robinson DL, Venton BJ, Heien MLAV, Wightman RM (2003) Detecting subsecond dopamine release with fast-scan cyclic voltammetry in vivo. Clinical chemistry 49:1763-1773.

Wang Y, Lee J-W, Oh G, Grady SR, McIntosh JM, Brunzell DH, Cannon JR, Drenan RM (2013) Enhanced synthesis and release of dopamine in transgenic mice with gain-of-function α6* nAChRs. Journal of Neurochemistry 129:315-327.

Xiao C, Nashmi R, McKinney S, Cai H, McIntosh JM, Lester HA (2009) Chronic nicotine selectively enhances α4β2* nicotinic acetylcholine receptors in the nigrostriatal dopamine pathway. J Neurosci 29:12428-12439.

Zhang T, Zhang L, Liang Y, Siapas AG, Zhou FM, Dani JA (2009) Dopamine signaling differences in the nucleus accumbens and dorsal striatum exploited by nicotine. J Neurosci 29:4035-4043.

Chapter 3

A collection of data relating to lynx1

My time in the Lester lab has been united by one common theme: the study of lynx1 and its effects on nicotinic receptors. I have studied lynx1 through many different methods. This chapter highlights experiments from early in my tenure in the Lester lab to demonstrate the breadth of experiments that I have undertaken. Previous studies of lynx1 had identified its interaction with α4β2 and α7 nicotinic receptors (Ibanez-Tallon et al., 2002; Miwa et al., 2006). My early experiments studied lynx1 in relation to these two nicotinic receptor subtypes.

Imaging of cells transfected with fluorescently tagged nicotinic receptors and lynx1

The first experiment I conducted was to transfect α4β2 nicotinic receptors with and without lynx1 into cultured cells to determine if there are differences in receptor localization when lynx1 is added. In order to visualize the nicotinic receptors, we used fluorescently tagged receptors that were developed in the Lester lab (Nashmi et al., 2003). These nicotinic receptors are tagged with various XFPs in the M3-M4 intracellular loop of the nicotinic receptor subunit.

α4GFP and β2 (unlabeled) nicotinic receptor subunits were transfected into COS7 cells from ATCC. We specifically chose COS7 cells because of their advantageous ER morphology. Typically, α4β2 receptors reside in the ER, with only a proportion of receptors making it to the surface of the cell (Nashmi et al., 2003). Therefore, we used COS7 cells which have a flat shape and a lacy ER morphology to be able to better visualize the ER (Snapp et al., 2003). For the COS7 experiments, we fixed the cells and immunostained with anti-GFP antibody to boost the

GFP signal from the receptors. We also used an anti-PDI antibody to show the ER (Figure 3.1) or anti-GM130 antibody to reveal the Golgi (Figure 3.2). The cells were imaged using confocal microscopy.

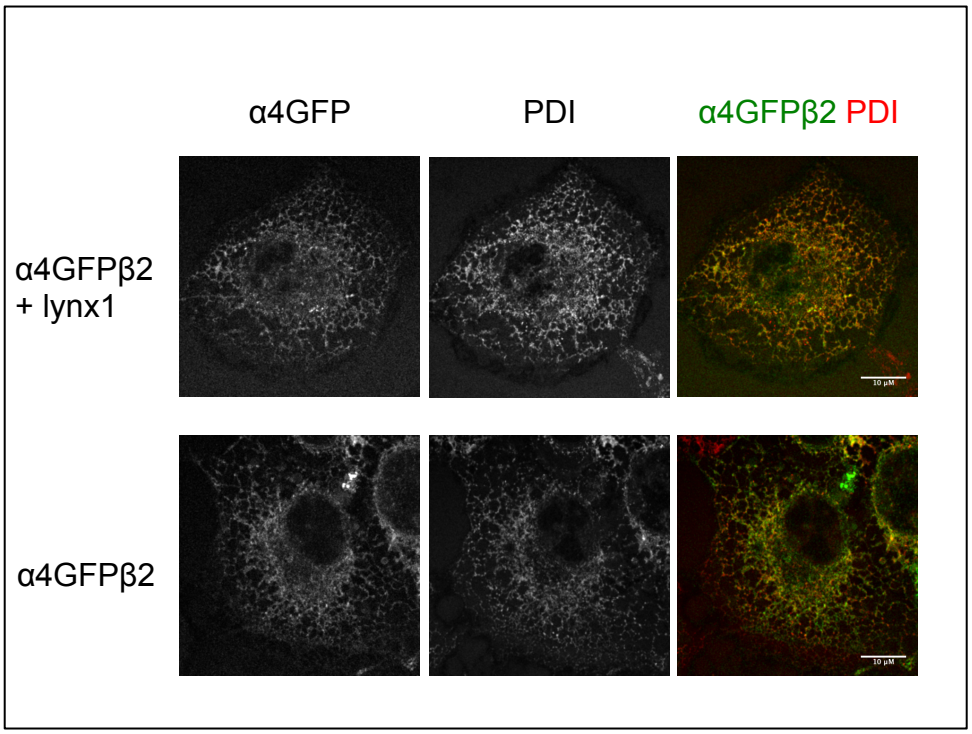

Figure 3.1: Confocal images of COS7 cells transfected with either α4GFPβ2 or α4GFPβ2 + lynx1, then immunostained for PDI. Scale bar is 10 μM.

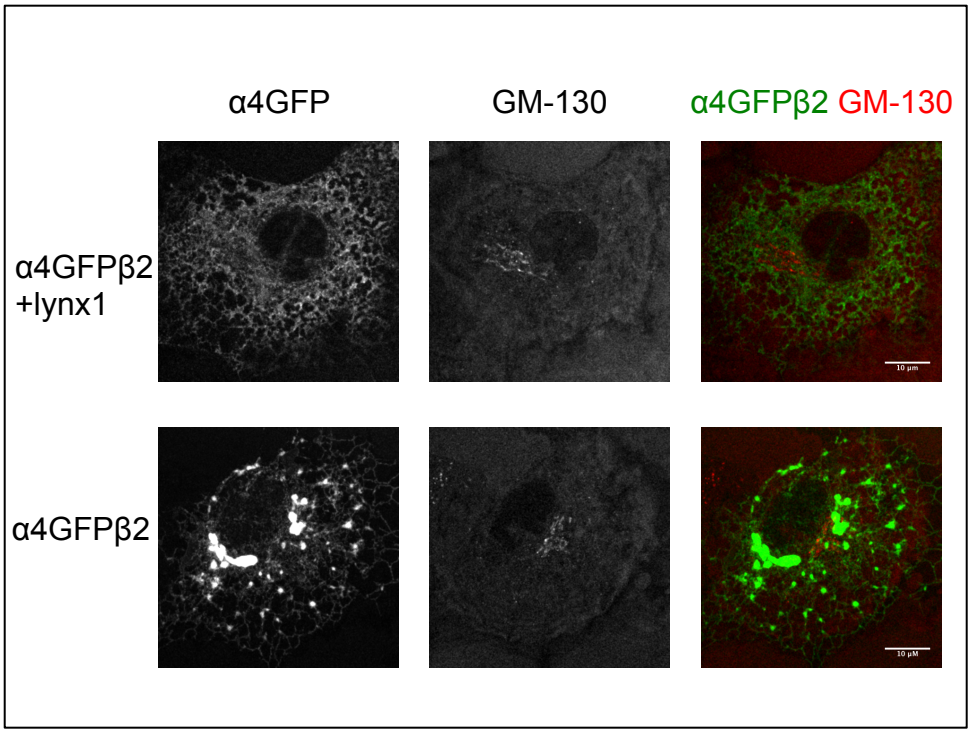

Figure 3.2: Confocal images of COS7 cells transfected with either α4GFPβ2 or α4GFPβ2 + lynx1, then immunostained for GM-130. Scale bar is 10 μM.

We did not note any overt differences when lynx1 was transfected into COS7 cells. Since these are neuronal nicotinic receptors, we thought that looking at neurons might be more advantageous. We used lynx1KO mice to generate cortical neurons that were lynx1WT, lynx1HET (heterozygous), and lynx1KO. After 6 days in culture, the neurons were transfected with α4GFP and β2 nicotinic receptor subunits using Lipofectamine 2000 and Nupherin Neuron. 24 hours post transfection, the neurons were live imaged with a confocal microscope. In addition to α4GFPβ2, we also transfected either pCs2-mCherry, dsRed-ER, or GALT-mCherry. We purposely took images that showed nearly the entire neuron, including the neurites, to see whether there were changes in those regions. In the neurons that were transfected with α4GFPβ2 in addition to pCs2-mCherry, the pCs2 marker is directed to the cell membrane, so the entire membrane is labeled (Figure 3.3). We did not note any differences in the membrane localization

of the α4GFPβ2 nicotinic receptors whether lynx1 is present, at half dose, or absent. We then used dsRed-ER and GALT-mCherry to compare whether there were changes in the receptors that were ER or Golgi localized (Figures 3.4 and 3.5). Again, we did not see any changes in receptor localization in the lynx1HET or lynx1KO neurons. These data suggest that lynx1 effects on α4GFPβ2 nicotinic receptors are not at the macroscopic level, but must be more subtle. Perhaps there are changes in receptor biogenesis, or there are changes in functional characteristics of the receptors when lynx1 is bound, but we did not detect them in this system.

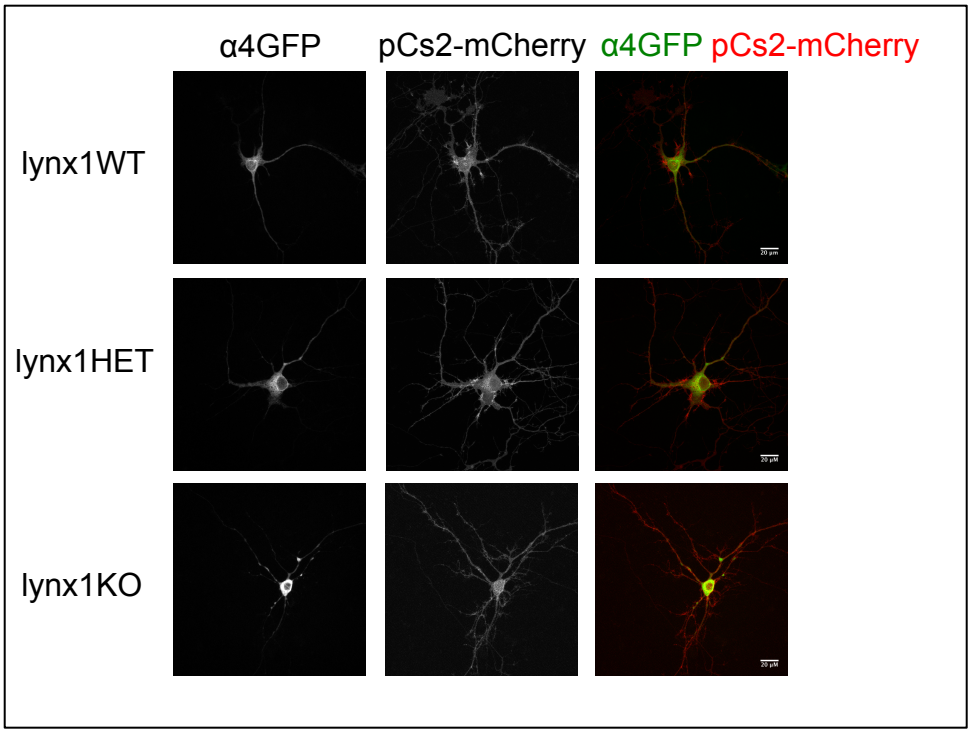

Figure 3.3: Cortical neurons from of lynx1WT, lynx1HET, and lynx1KO mice transfected with α4GFPβ2 and pCs2-mCherry. Scale bar is 10 μm.

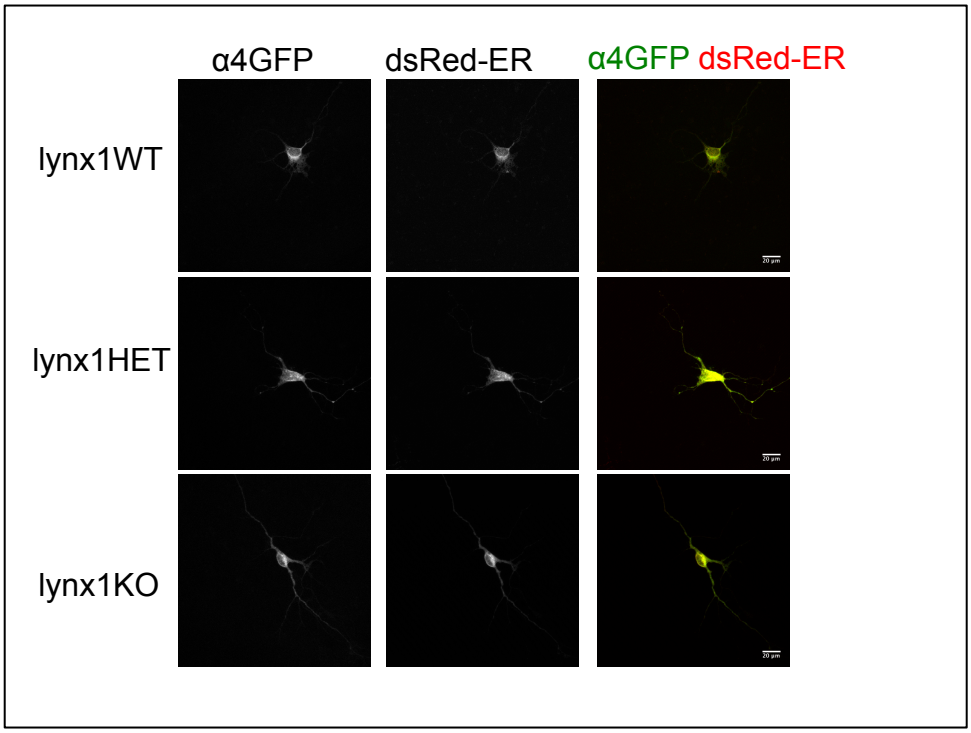

Figure 3.4: Cortical neurons from lynx1WT, lynx1HET, and lynx1KO mice transfected with α4GFPβ2 and dsRed-ER. Scale bar is 10 μm.

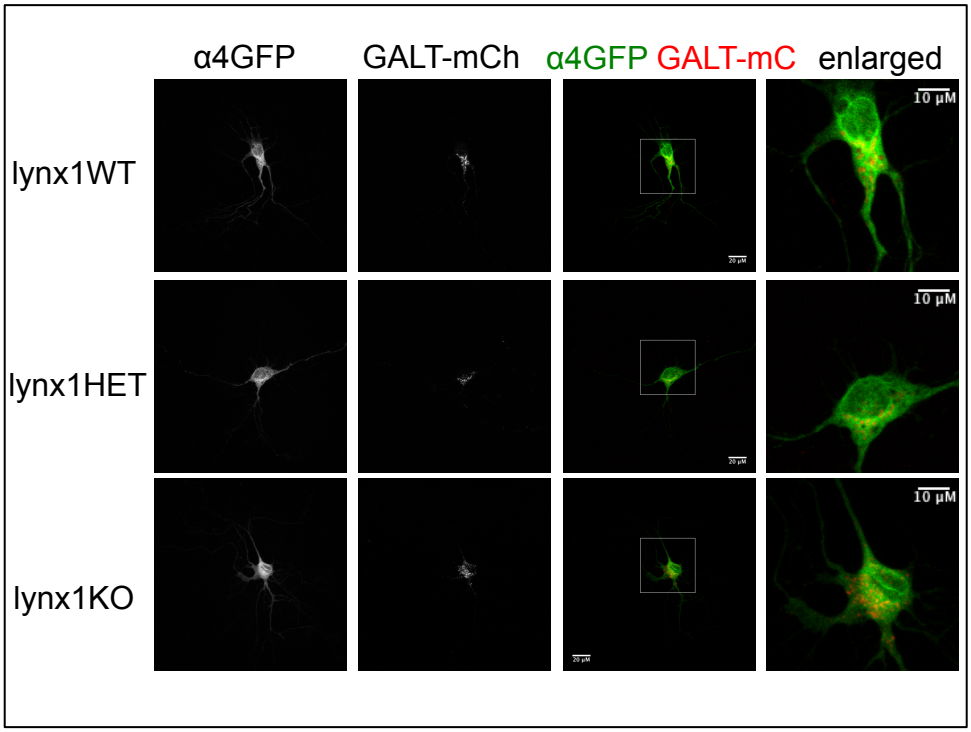

Figure 3.5: Cortical neurons from of lynx1WT, lynx1HET, and lynx1KO mice transfected with α4GFPβ2 and GALT-mCherry. Scale bar is 10 μm.

Electrophysiological Recordings in the Medial Habenula

Previous studies have indicated that there are functional changes in nicotinic receptors in the lynx1KO mice (Miwa et al., 2006). In that study, various concentrations of nicotine were used to establish a concentration response curve for nicotine in medial habenula slices from lynx1KO mice. The medial habenula is a brain region that is thought to regulate nicotine intake (Fowler et al., 2011). The data showed that in the lateral edge of the medial habenula the concentration response curve for nicotine was shifted to the left, and the peak response was larger when lynx1 was knocked out (Miwa et al., 2006).

One phenotype that has been reported in the lynx1KO mice is the development of vacuoles in the dorsal striatum and other regions (Miwa et al., 2006). However, in the Kobayshi et al. paper, we showed data that the lynx1HET mice do not develop these vacuoles (Kobayashi et al., 2014). This led us to question whether there was a difference in the response to application of nicotine in the lynx1HET mice. We asked whether functionally the lynx1HET mice resemble the lynx1KO or the lynx1WT mice. A dose of 20 μM nicotine was chosen as it had the maximal difference between lynx1KO and lynx1WT in a previous study (Miwa et al., 2006). Patch clamp electrophysiology traces showing the response to 20 μM nicotine are shown in Figure 3.6A. Figure 3.6B shows the recording set up, with the patch pipette to the left and the puffer pipette coming from the bottom right corner. The lateral edge of the medial habenula is visible as a line along the left corner of the picture. It is important to note that recordings are consistently taken from the same region of the medial habenula, as different nicotinic receptor subtypes are located in the various regions of the medial habenula (Lester and collaborators, unpublished data). We found that with 20 μM nicotine the lynx1HET cells had a similar peak response and net current as the lynx1KO, but showed a statistically significant difference from lynx1WT animals (Figure 3.6C and D). The values for peak amplitude (in pA) were: lynx1WT 21.5 ± 5.1, lynx1HET 77.1 ± 15.0, and lynx1KO 68.2 ± 11.7. Using ANOVA on Ranks, with a post-hoc Dunn's Test, the peak response p-value was $p = 0.010$, with both lynx1KO and lynx1HET different from lynx1WT, but not different from each other. The values for net charge (in pA x ms) were: lynx1WT 6718.8 ± 2545.5, lynx1HET 60165 ± 14967, and lynx1KO 60874 ± 13006. The net change data had a p-value of $p = 0.003$, again with lynx1KO and lynx1HET different from lynx1WT, but not different from each other.

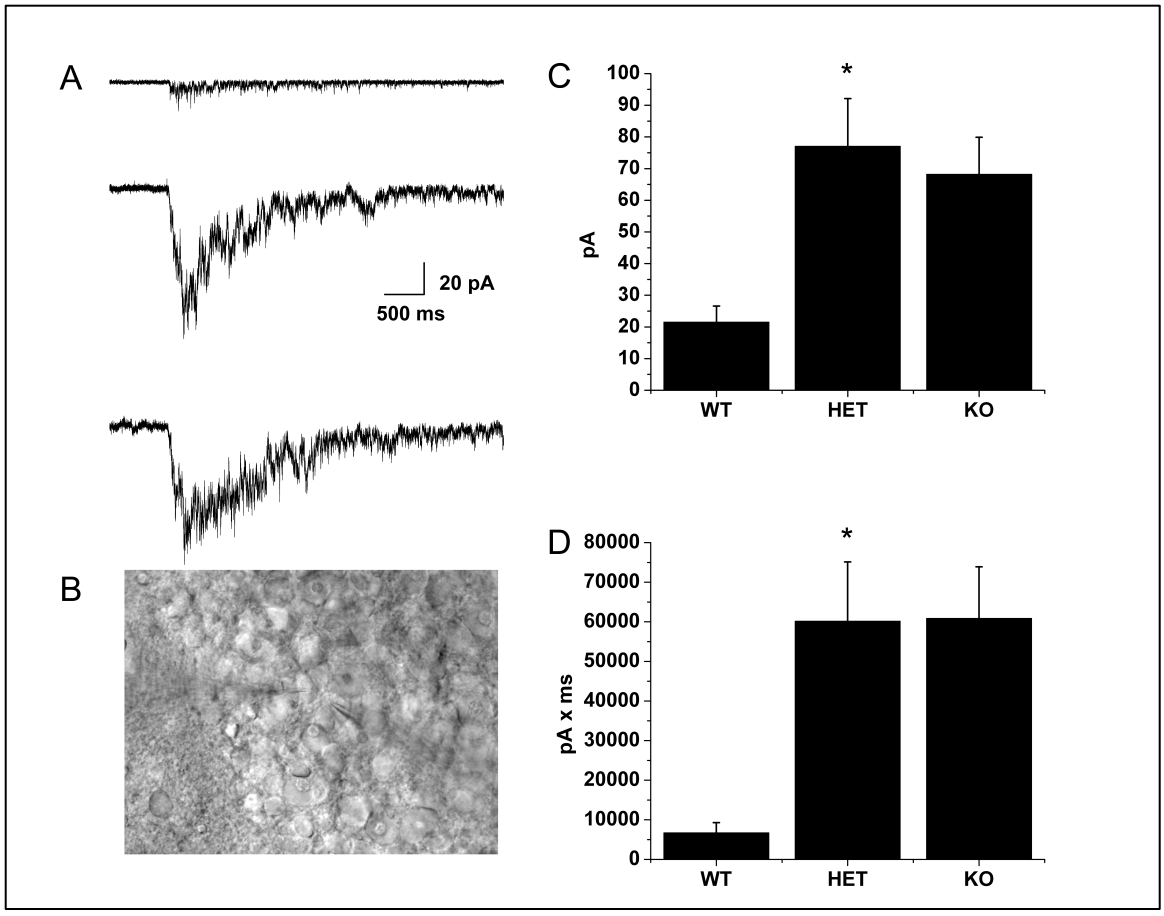

Figure 3.6: A) Traces showing response to 20 μM of nicotine. Top trace is lynx1WT, middle is lynx1HET, and bottom is lynx1KO. Scale bar is 20 pA and 500 ms. B) Picture of cell from lateral edge of medial habenula showing patch pipette to left and puffer pipette from bottom right. C) Graph of average peak response. WT is significantly different from HET and KO. D) Graph of average net charge; WT is significantly different from HET and KO. For C) and D) the number of cells recorded is 8 lynx1WT, 22 lynx1HET, and 15 lynx1KO.

The medial habenula data was reassuring, as it confirmed the differences between the lynx1KO and lynx1WT that were previously published (Miwa et al., 2006). It also demonstrated that the lynx1HET mice showed a similar response as the lynx1KO mice. A partial reduction of lynx1 actually had the same effect as complete removal of lynx1, which was unexpected. Another recent study from our lab (Kobayashi et al., 2014) showed that there is an approximately 50% reduction of lynx1 RNA transcripts and protein in the lynx1HET mice. This suggests that the change in lynx1HET peak response is not due to complete loss of lynx1. Even though a half dose

of lynx1 is sufficient to protect from formation of vacuoles, it does not alter the functional characteristics of the nicotinic receptors in the medial habenula.

lynx1 and the development of inhibitory circuits

Another area of study that I have pursued is the role of lynx1 in development. Studies of the lynx1KO mouse have confirmed that lynx1 is important for the close of the critical period for vision (Morishita et al., 2010). The effects of lynx1 in the visual system indicate that lynx1 has a critical role in circuit development in that region. We hypothesized that it may be important in other brain regions as well. α7 nicotinic receptors are important for circuit development in the hippocampus, particularly in the development of inhibition (Liu et al., 2006). lynx1 can interact with α7 nicotinic receptors, presenting the possibility that lynx1 is an upstream regulator of inhibitory circuit development in the hippocampus. To test this we conducted some preliminary electrophysiological studies in the CA3 region of the hippocampus in the lynx1KO mice.

The electrophysiological recordings were conducted in the lynx1WT, lynx1HET, and lynx1KO mice. This region was chosen due to its high lynx1 expression (Miwa et al., 1999). Additionally, α7 nAChRs are highly expressed in the hippocampus, as revealed by in situ hybridization and α-Bungarotoxin binding (Seguela et al., 1993; Orr-Urtreger et al., 1997). We believed that recordings in this region would have the best chance of revealing an effect of lynx1 due to the normally high expression. We measured EPSCs to determine whether there were any changes in hippocampal circuits (Figure 3.7A). Patch clamp recordings were made on CA3 neurons. The internal solution had a chloride concentration of 5 mM (Figure 3.7B). EPSCs were measured by taking 5 minute recordings (Figures 3.8 and 3.9). The values for peak amplitude (in pA) at p5-6 were lynx1WT 16.8 ± 2.0, lynx1HET 20.5 ± 2.3, and lynx1KO 17.9 ± 3.9. The values for peak amplitude (in pA) at p8-10 were lynx1WT 18.2 ± 1.9, lynx1HET 22.1 ± 2.3, and lynx1KO 15.9 ±

4.9. The rate of EPSCs was recorded as well. The frequency values in Hz for p5-6 were lynx1WT 1.5 ± 0.2, lynx1HET 1.4 ± 0.3, and lynx1KO 1.0 ± 0.2. The frequency values in Hz for p8-10 were lynx1WT 2.0 ± 0.5, lynx1HET 1.4 ± 0.3, and lynx1KO 1.7 ± 0.5. No significant differences of lynx1KO were found in any of these recordings.

The recordings for EPSCs were conducted at -65 mV. However, during the experiment, we shifted the cell to a holding potential of -50 mV in order to reveal IPSCs. We noted large IPSCs which approached 100 pA in several of the lynx1 KO cells. We did not see any similar currents in WT animals (Figure 3.10). We do not know the origin of these currents. They are only revealed at a holding current of -50 mV or more depolarized, suggesting that these currents are inhibitory synaptic currents. Future studies could be done to elucidate the role of these currents. If confirmed, they may indicate that lynx1KO alters synaptic inhibition in the hippocampus. Unfortunately we did not complete these studies, but they may be interesting to pursue in the future.

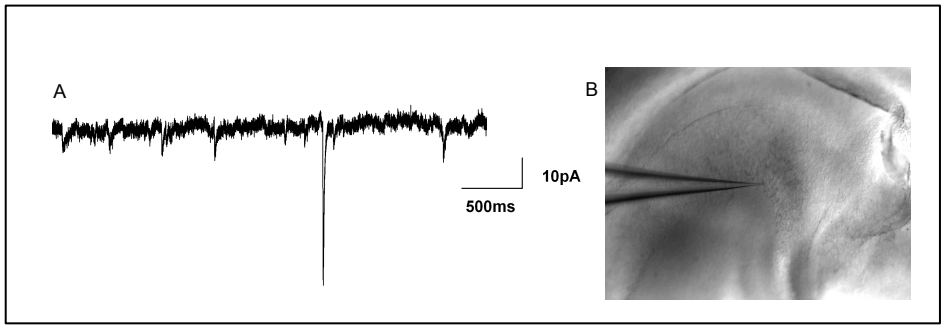

Figure 3.7: A) Sample trace showing EPSCs. B) Image showing hippocampus CA3 with patch pipette visible.

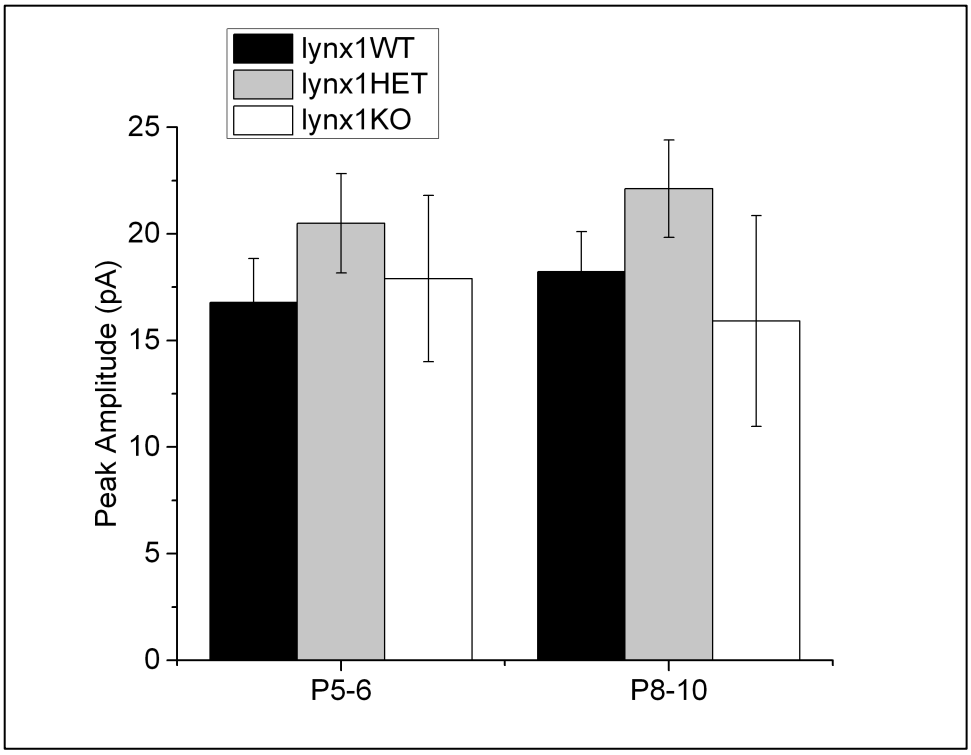

Figure 3.8: Average peak amplitude of EPSCs recorded in lynx1WT, lynx1HET, and lynx1KO hippocampal slices from animals that were either p5-6 or p8-10. The number of cells for p5-6 are lynx1WT 6, lynx1HET 7, and lynx1KO 3. The number of cells for p5-6 are lynx1WT 15, lynx1HET 5, and lynx1KO 4.

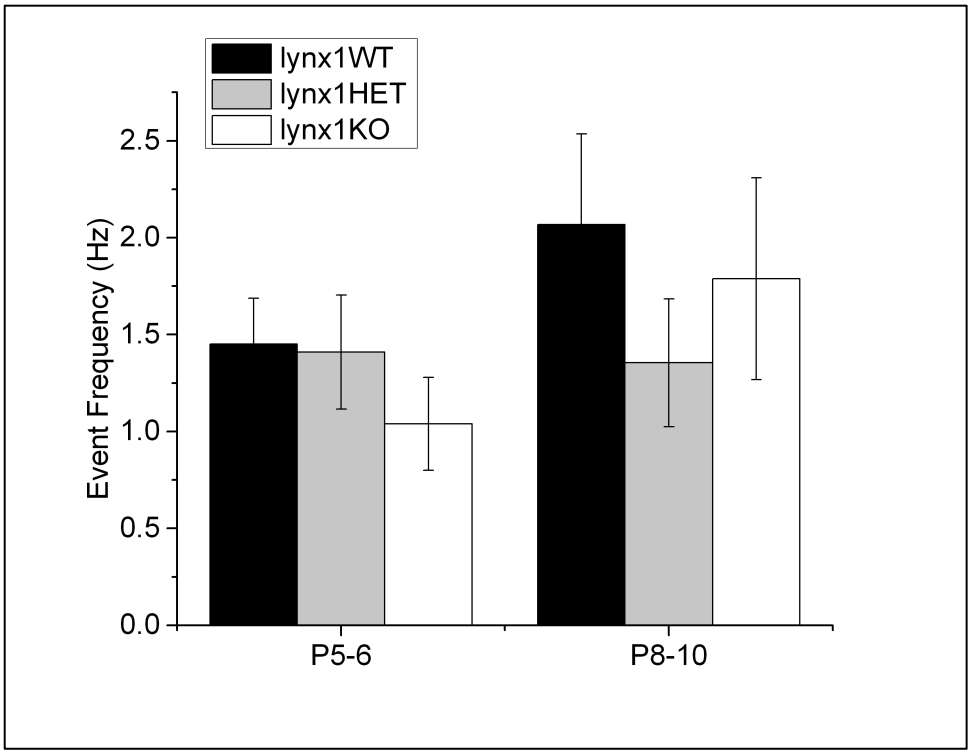

Figure 3.9: Average frequency of EPSCs recorded in lynx1WT, lynx1HET, and lynx1KO hippocampal slices from animals that were either p5-6 or p8-10. Cell numbers as in Figure 3.8.

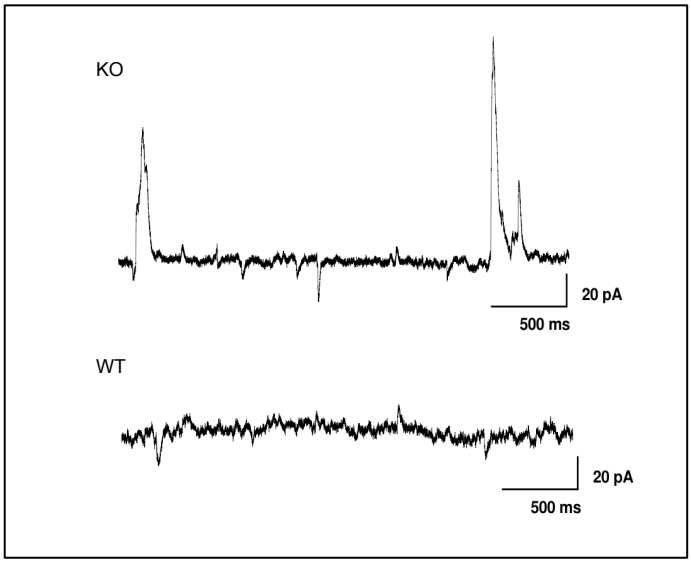

Figure 3.10: Traces taken with holding current switched to -50 mV; the internal pipette solution contained 5 mM Cl^-. In the lynx1KO trace (top) large upward currents are present. These were not observed in the lynx1WT mice (bottom). Scale is 20 pA and 500 ms.

The electrophysiological recordings in the hippocampus indicated that there is likely altered inhibition in those circuits. To explore the in vivo effects of altered inhibition in the hippocampus of lynx1 KO mice, we used a established mouse behavioral assay, prepulse inhibition (PPI) (Amann et al., 2010). PPI behavior is altered in several neuropsychiatric diseases, including schizophrenia, autism, and obsessive-compulsive disorder (Geyer and Dulawa, 2003). PPI measures sensorimotor gating; it is mediated by the brainstem and regulated by the hippocampus. The pre-pulse is a tone of either 5 or 15 dB above background played before a loud 120 dB tone. The 120 dB tone will cause the animal to startle, but the prepulse will generally decrease the size of the startle response.

We were not able to use C57Bl/6 mice for this experiment because of their age-related hearing loss, so we backcrossed the lynx1KO mice to C3H mice and used N1/F1 animals for this experiment. We found that PPI was unaffected by lynx1KO, but we did find a decrease in the acoustic startle response to a single tone (Figures 3.11 and 3.12). Using ANOVA on Ranks, the p-value for startle was $p =< 0.001$; post-hoc testing with Dunn's test showed that lynx1KO was significantly decreased from lynx1WT and lynx1HET. This reduction in startle magnitude suggests that there is increased inhibition in the lynx1KO animals (Koch, 1999). This effect is not likely due to habitation, because the response to the first few pulses was not significantly different to the response to the last few pulses in the lynx1KO mice.

The hippocampal recordings and the PPI experiments suggest that lynx1KO does affect the development of inhibition. This is not surprising, as there are several types of evidence that connect lynx1 to inhibition. The paper by Morishita et al. that established the role of lynx1 in critical period development suggested that lynx1KO mice have an altered excitatory to inhibitory balance with increased excitation (Morishita et al., 2010). Mice lacking the transporter NKCC1

do not develop mature inhibitory networks, and lynx1 protein expression is reduced in these mice (Pfeffer et al., 2009). lynx1 acts as a brake on nicotinic receptors in particular, but it appears that knocking out lynx has wide consequences on the development of neuronal circuits.

Conclusion

We have used many modalities to study the effects of lynx1, from biochemistry to behavior, from imaging to electrophysiology. The electrophysiological studies in the hippocampus and PPI experiments showed promising results. Both indicated a role for lynx1 in the development of inhibition. This agrees with a previous study on lynx1KO mice, which found altered excitatory to inhibitory balance in the visual cortex (Morishita et al., 2010). lynx1 clearly plays an important role in development, particularly the development of inhibitory circuits. More studies are needed to fully elucidate the function of lynx1 in this context.

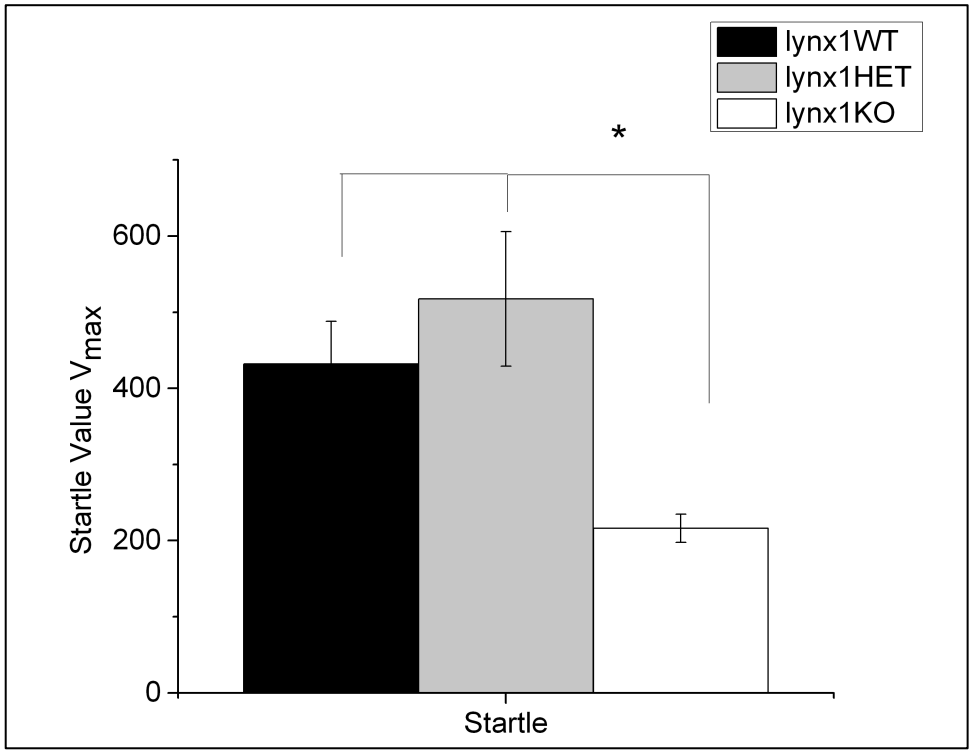

Figure 3.11: Startle value to 120 dB tone. lynx1KO mice startle significantly less than lynx1WT or lynx1HET mice.

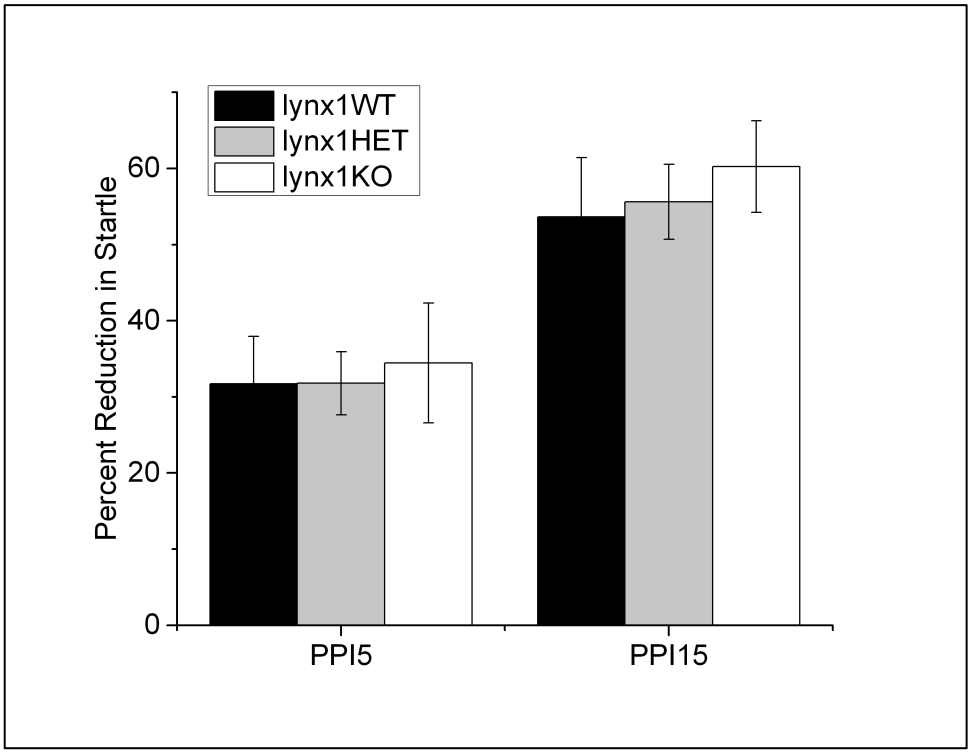

Figure 3.12: PPI as a percent reduction of startle following a prepulse of either 5 or 15 dB. There was no significant difference between the genotypes.

References

Amann LC, Gandal MJ, Halene TB, Ehrlichman RS, White SL, McCarren HS, Siegel SJ (2010) Mouse behavioral endophenotypes for schizophrenia. Brain Research Bulletin 83:147-161.

Fowler CD, Lu Q, Johnson PM, Marks MJ, Kenny PJ (2011) Habenular α5 nicotinic receptor subunit signalling controls nicotine intake. Nature.

Geyer MA, Dulawa SC (2003) Assessment of murine startle reactivity, prepulse inhibition, and habituation. Current protocols in neuroscience / editorial board, Jacqueline N Crawley [et al] Chapter 8:Unit 8.17.

Ibanez-Tallon I, Miwa JM, Wang HL, Adams NC, Crabtree GW, Sine SM, Heintz N (2002) Novel modulation of neuronal nicotinic acetylcholine receptors by association with the endogenous prototoxin lynx1. Neuron 33:893-903.

Kobayashi A, Parker RL, Wright AP, Brahem H, Ku P, Oliver KM, Lester HA, Miwa JM (2014) lynx1 Supports Neuronal Health in the Mouse Dorsal Striatum During Aging: an Ultrastructural Investigation. Journal of Molecular Neuroscience In Press.

Koch M (1999) The neurobiology of startle. Progress in neurobiology 59:107-128.

Liu Z, Neff RA, Berg DK (2006) Sequential interplay of nicotinic and GABAergic signaling guides neuronal development. Science 314:1610-1613.

Miwa JM, Ibanez-Tallon I, Crabtree GW, Sanchez R, Sali A, Role LW, Heintz N (1999) lynx1, an endogenous toxin-like modulator of nicotinic acetylcholine receptors in the mammalian CNS. Neuron 23:105-114.

Miwa JM, Stevens TR, King SL, Caldarone BJ, Ibanez-Tallon I, Xiao C, Fitzsimonds RM, Pavlides C, Lester HA, Picciotto MR, Heintz N (2006) The Prototoxin lynx1 Acts on

Nicotinic Acetylcholine Receptors to Balance Neuronal Activity and Survival In Vivo. Neuron 51:587-600.

Morishita H, Miwa J, Heintz N, Hensch T (2010) Lynx1, a cholinergic brake, limits plasticity in adult visual cortex. Science 330:1238-1240.

Nashmi R, Dickinson ME, McKinney S, Jareb M, Labarca C, Fraser SE, Lester HA (2003) Assembly of a4b2 nicotinic acetylcholine receptors assessed with functional fluorescently labeled subunits: effects of localization, trafficking, and nicotine-induced upregulation in clonal mammalian cells and in cultured midbrain neurons. J Neurosci 23:11554-11567.

Orr-Urtreger A, Goldner FM, Saeki M, Lorenzo I, Goldberg L, De Biasi M, Dani JA, Patrick JW, Beaudet AL (1997) Mice deficient in the a7 neuronal nicotinic acetylcholine receptor lack a-bungarotoxin binding sites and hippocampal fast nicotinic currents. J Neurosci 17:9165-9171.

Pfeffer CK, Stein V, Keating DJ, Maier H, Rinke I, Rudhard Y, Hentschke M, Rune GM, Jentsch TJ, Hubner CA (2009) NKCC1-dependent GABAergic excitation drives synaptic network maturation during early hippocampal development. J Neurosci 29:3419-3430.

Seguela P, Wadiche J, Dineley-Miller K, Dani JA, Patrick JW (1993) Molecular cloning, functional properties, and distribution of rat brain a7: a nicotinic cation channel highly permeable to calcium. J Neurosci 13:596-604.

Snapp EL, Hegde RS, Francolini M, Lombardo F, Colombo S, Pedrazzini E, Borgese N, Lippincott-Schwartz J (2003) Formation of stacked ER cisternae by low affinity protein interactions. The Journal of Cell Biology 163:257-269.

Conclusion

The cholinergic signaling system, which consists of both muscarinic and nicotinic receptors, is a complex system. Narrowing the focus to nicotinic receptors alone, there are still multiple subunits and many possible combinations of these subunits with unique properties. Compounding this complexity, different brain regions contain unique subsets of nicotinic receptors (Gotti et al., 2009). The previous chapters have presented my studies of neuronal nicotinic receptors and their regulation by lynx1.

lynx1 is a protein that modulates nicotinic receptors via interaction with the extracellular portion of the nicotinic receptor (Miwa et al., 1999). However, lynx1 is just one member of a family of proteins which affect nicotinic receptors (Tekinay et al., 2009; Miwa et al., 2012). When lynx1 is knocked out, there may be other family members present which can compensate for its loss. Additionally, lynx1 effects may be different on the different nicotinic receptor subtypes. Due to the complexity of this system, it is easy to understand how the effects of lynx1 might be difficult to parse out.

We tried to deal with the complexity of the system by studying the effects of lynx1 on the α6 nicotinic receptor subunit. This appeared to be a favorable system to use because of the limited expression of α6* nicotinic receptors, which are only in a few regions of the brain (Whiteaker et al., 2000; Mackey et al., 2012). With our lab having previously made α6L9'S mice, which have hypersensitive α6* nicotinic receptors, we also possessed a tool with which to study the interaction between lynx1 and α6* nicotinic receptors. Due to the hypersensitive α6* nicotinic receptors in these mice, the function of α6* nicotinic receptors is more easily observed. With

these α6L9'S mice and α-CTX MII, a toxin that specifically blocks α6* nicotinic receptors, we thought that we had good tools to study the effect of lynx1 on α6.

Once we crossed the lynx1KO mice to the α6L9'S mice, we began behavioral studies. We examined their ability to habituate to novel environments and their home cage activity. We immediately observed that there were very few lynx1KO α6L9'S mice that were hyperactive, and it appeared that these mice did habituate to a novel environment. However, we did not properly account for the bimodal distribution of the α6L9'S mice in analyzing the results of the experiment. In fact, only about 50% of the α6L9'S mice are hyperactive (Drenan et al., 2008). This made it extremely difficult to get statistical significance, and in the end we were not able to. This turned out to be one shortcoming of this model to study lynx1. It would have been much easier to determine significance if there was less variability in the α6L9'S mice.

We have shown that lynx1 does have effects on nicotinic receptors, but these effects are necessarily subtle and difficult to isolate. While it is important that there is a way to control the cholinergic system setpoint by having a protein such as lynx1, it would be maladaptive for lynx1 to cause large swings in cholinergic excitability. In fact, a previous study showed that knocking out the α4 nicotinic receptor subunit had some effects on the α6L9'S mice, but did not result it complete loss of hyperactivity (Drenan et al., 2010). We would expect that knocking out lynx1, a modulator of nicotinic receptors, would have a smaller effect than knocking out an entire nicotinic receptor subunit.

One advantage for this project was that it led to the use of a variety of different techniques, from biochemistry, to mouse behavior, electrophysiology, and voltammetry. These are all valuable techniques that I can take with me and use for future endeavors. I think that this project was also

a good learning experience because of the many challenges that I faced along the way. I have a better understanding of how to select a project and how to take that project to a successful ending. I know that these experiences will serve me well in the future.

References

Drenan RM, Grady SR, Steele AD, McKinney S, Patzlaff NE, McIntosh JM, Marks MJ, Miwa JM, Lester HA (2010) Cholinergic modulation of locomotion and striatal dopamine release is mediated by α6α4* nicotinic acetylcholine receptors. J Neurosci 30:9877-9889.

Drenan RM, Grady SR, Whiteaker P, McClure-Begley T, McKinney SR, Miwa J, Bupp S, Heintz N, McIntosh JM, Bencherif M, Marks MA, Lester HA (2008) *In Vivo* Activation of Midbrain Dopamine Neurons via Sensitized, High-Affinity α6* Nicotinic Acetylcholine Receptors. Neuron 60:123-136.

Gotti C, Clementi F, Fornari A, Gaimarri A, Guiducci S, Manfredi I, Moretti M, Pedrazzi P, Pucci L, Zoli M (2009) Structural and functional diversity of native brain neuronal nicotinic receptors. Biochemical pharmacology 78:703-711.

Mackey ED, Engle SE, Kim MR, O'Neill HC, Wageman CR, Patzlaff NE, Wang Y, Grady SR, McIntosh JM, Marks MJ, Lester HA, Drenan RM (2012) α6* Nicotinic Acetylcholine Receptor Expression and Function in a Visual Salience Circuit. J neurosci 32:10226-10237.

Miwa JM, Lester HA, Walz A (2012) Optimizing cholinergic tone through lynx modulators of nicotinic receptors: implications for plasticity and nicotine addiction. Physiology 27:187-199.

Miwa JM, Ibanez-Tallon I, Crabtree GW, Sanchez R, Sali A, Role LW, Heintz N (1999) lynx1, an endogenous toxin-like modulator of nicotinic acetylcholine receptors in the mammalian CNS. Neuron 23:105-114.

Tekinay AB, Nong Y, Miwa JM, Lieberam I, Ibanez-Tallon I, Greengard P, Heintz N (2009) A role for LYNX2 in anxiety-related behavior. Proc Natl Acad Sci U S A 106:4477-4482.

Whiteaker P, McIntosh JM, Luo S, Collins AC, Marks MJ (2000) ^{125}I-α-conotoxin MII identifies a novel nicotinic acetylcholine receptor population in mouse brain. Molecular Pharmacology 57:913-925.

Appendix: Fast Scan Cyclic Voltammetry Methods

Slices are made following the same procedure as for electrophysiology.

Electrode Fabrication:

Electrodes were fabricated using carbon fiber (7 μM, unsized from Goodfellow) and glass without filament from Sutter (B150-86-10). One carbon fiber was pulled through a glass micropipette using a vacuum, which was then pulled into two electrodes on a Sutter Puller. The carbon fibers were trimmed and the electrodes dipped into epoxy for 7 minutes and then quickly rinsed in acetone.

The epoxy is a four component epoxy, ordered from Polysciences. The epoxy components are: DER expoxy resin cat #02943, ERL 4221 cat #24738, Nonnenylsuccinic anhydride cat #01542, and 2-Dimethylamino ethanol cat #01458. To make the epoxy, 4.10 g ERL 4221, 5.90 g NSA, and 1.43 g DER are combined and mixed in a glass scintillation vial. Then 120 μL of DMAE is added to the mixture.

Electrodes were baked overnight at 80 °C to cure the epoxy, and the carbon fiber was trimmed once more before use if needed. The glass pipette was filled with 150 mM KCl prior to the experiment. Often the electrodes were filled with the KCl solution in advance to ensure that they were not leaking. Each individual carbon fiber electrode (CFE) was tested prior to use to ensure that it had a minimum sensitivity of 80 nA, but did not saturate the amplifier (max of amplifier was 200 nA). If needed the electrodes can be dipped in a mixture of isopropanol and carbon power to clean them.

Recordings:

Recordings were made with an Axon Multiclamp 700B Amplifier and recorded using Clampex 9, both from Molecular Devices Axon, Sunnyvale, CA. The amplifier gain settings were adjusted to voltage clamp feedback resistor 50 MΩ, external command sensitivity of 100 mV/V, current clamp feedback resistor 50 mΩ, and external command sensitivity 20 nA/V. The protocol screen shots are at the end of this document. Briefly, the voltage is swept from -400 mV to +1000 mV to -400 mV, at a rate of 300 mV/ ms. The sampling interval is 20 μs, so the sampling frequency is 50 kHz. Each sweep is 20 ms with 100 ms between sweeps.

The carbon fiber electrode was placed in the dorsal striatum, with the tip of the carbon fiber just below the surface of the slice. The animals used in these experiments were 18-27 weeks old. Slices were prepared in a similar fashion as for electrophysiology, except the slices were 300 μM thick, and were taken from the striatum. The stimulating electrode was placed about 100-200 μM from the carbon fiber electrode. A bipolar stimulating electrode was used. The pulse was sufficient to elicit maximal stimulation, and the 2p and 4p stimuli were delivered at 100 Hz. The slices were given time to adjust to the rig, the values would tend to stabilize after 30 minutes. Different regions of the striatum are tried until a large response is found. The stimulus application was limited to limit desensitization, therefore the slice was not stimulated more than every 2.5 minutes.

A dopamine standard was made by diluting dopamine HCl (Sigma H8502) into 0.1 N perchloric acid. A 1 mM solution of dopamine was made and aliquoted to be frozen at -20 °C. At the end of the experiment the carbon fiber was submerged in solution and a new file was started. A few minutes of recording were done in regular solution, then the solution was switched to 1 μM

dopamine solution, freshly made up in ACSF. During the analysis phase, the sweeps before dopamine (control) were averaged together. The sweeps with 1 μM dopamine were averaged together as well, with sweeps during the transition discarded. The average control trace was subtracted from the averaged 1 μM trace. The value of the subtracted trace was the 1 μM calibration factor.

Data Analysis:

The peak response was measured, and a single exponential fit was used to determine tau. See (Perez et al., 2008; Perez et al., 2013). To analyze the data in clampfit, the file is opened and the cursor was moved to the following positions: Cursor 1: 0.38 ms, Cursor 2:3.18 ms. Cursor 3 8.38 ms, and Cursor 4 9.18 ms.

Click the select sweeps button and select approximately 60 sweeps, with about 10 before your stimulus and the rest following. Set the statistics so that the peak is calculated between cursors 3 and 4 and the baseline is between cursors 1 and 2. Go to the results page and make a graph that charts trace number by size of response. Note which trace number the peak occurs at, and the last baseline trace number before the response is seen.

Go back to data file. Hit arithmetic. Add a single trace, then set that new trace as the peak response trace minus the baseline traces. Ex: t9081=t3004-t2999 for a stimulation where the peak response is in sweep 3004.

Check cursors 3 and 4 so that the peak of your new trace is between them. Then calculate statistics again. In the results page the peak of your new trace (using our example trace 9081) is the peak DA release. Copy that value and save it.

You can then graph the results again, with peak value versus time. Fit a single exponential decay to this graph in clampfit graph window to get the tau. Save this value.

Finally, go back to data window. If you would like to save your voltammogram you may hit select sweeps again, and select only your added trace. Then save this trace as a separate file.

It is ideal is to collect data from two sites per animal.

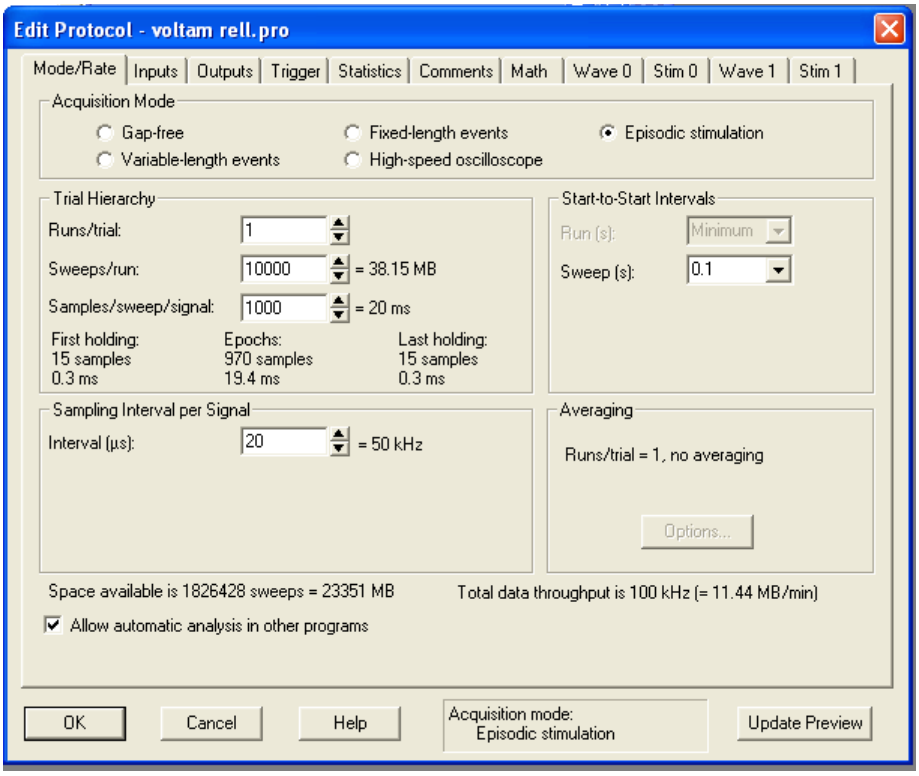

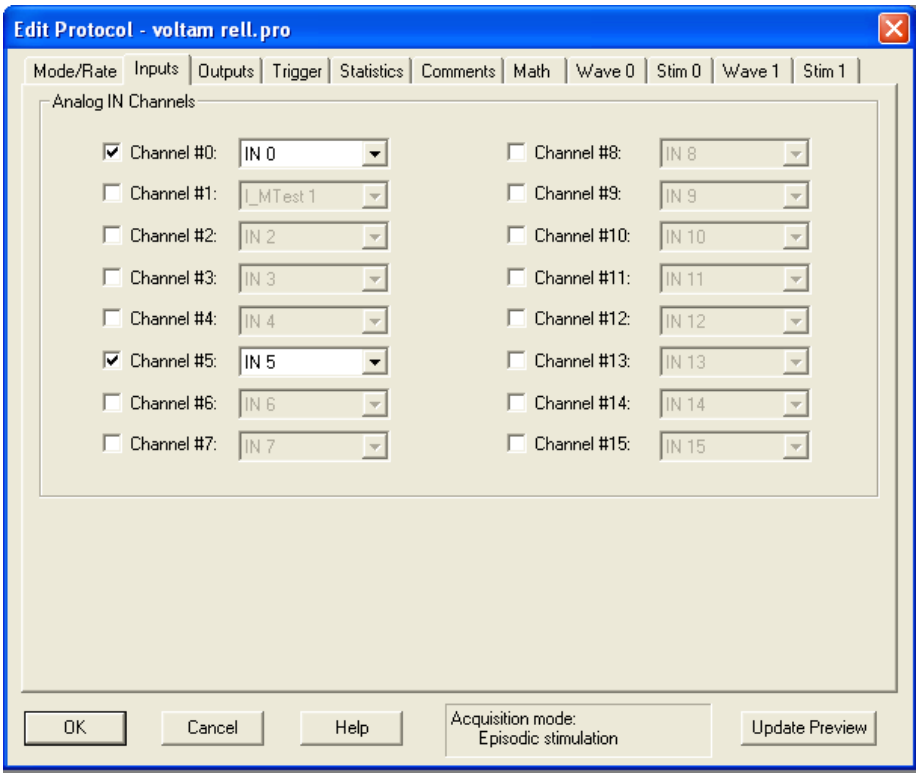
Edit Protocol - voltam rell.pro
Mode/Rate
Inputs
Outputs
Trigger
Statistics
Comments
Math
Wave 0
Stim 0
Wave 1
Stim 1
Analog IN Channels
Channel #0: IN 0
Channel #1: I_MTest 1
Channel #2: IN 2
Channel #3: IN 3
Channel #4: IN 4
Channel #5: IN 5
Channel #6: IN 6
Channel #7: IN 7
Channel #8: IN 8
Channel #9: IN 9
Channel #10: IN 10
Channel #11: IN 11
Channel #12: IN 12
Channel #13: IN 13
Channel #14: IN 14
Channel #15: IN 15
OK
Cancel
Help
Acquisition mode:
Episodic stimulation
Update Preview

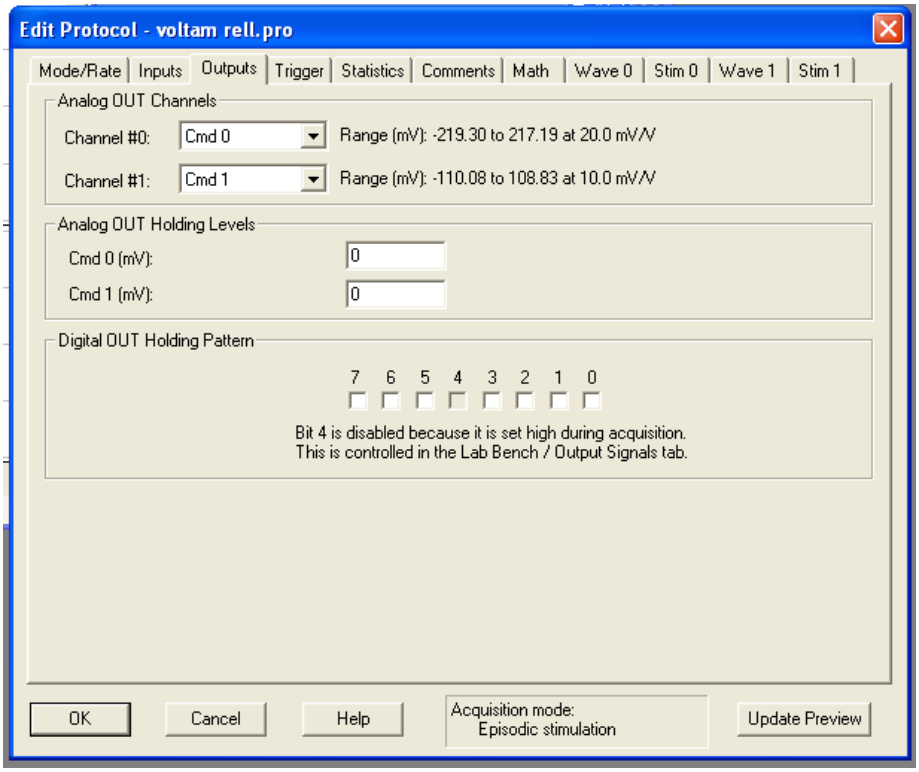
Edit Protocol - voltam rell.pro
Mode/Rate
Inputs
Outputs
Trigger
Statistics
Comments
Math
Wave 0
Stim 0
Wave 1
Stim 1
Analog OUT Channels
Channel #0: Cmd 0
Range (mV): -219.30 to 217.19 at 20.0 mV/V
Channel #1: Cmd 1
Range (mV): -110.08 to 108.83 at 10.0 mV/V
Analog OUT Holding Levels
Cmd 0 (mV): 0
Cmd 1 (mV): 0
Digital OUT Holding Pattern
7 6 5 4 3 2 1 0
Bit 4 is disabled because it is set high during acquisition.
This is controlled in the Lab Bench / Output Signals tab.
OK
Cancel
Help
Acquisition mode:
Episodic stimulation
Update Preview

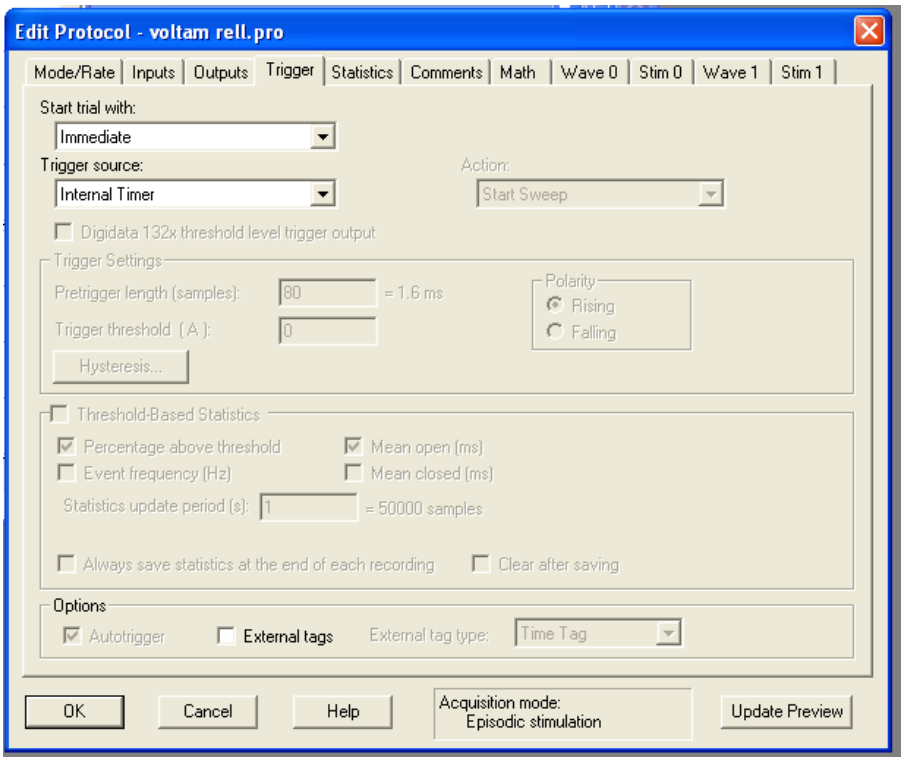
Edit Protocol - voltam rell.pro
Mode/Rate
Inputs
Outputs
Trigger
Statistics
Comments
Math
Wave 0
Stim 0
Wave 1
Stim 1
Start trial with:
Immediate
Trigger source:
Internal Timer
Action:
Start Sweep
Digidata 132x threshold level trigger output
Trigger Settings
Pretrigger length (samples):
80
= 1.6 ms
Trigger threshold (A):
0
Hysteresis...
Polarity
Rising
Falling
Threshold-Based Statistics
Percentage above threshold
Event frequency (Hz)
Mean open (ms)
Mean closed (ms)
Statistics update period (s):
1
= 50000 samples
Always save statistics at the end of each recording
Clear after saving
Options
Autotrigger
External tags
External tag type:
Time Tag
OK
Cancel
Help
Acquisition mode:
Episodic stimulation
Update Preview

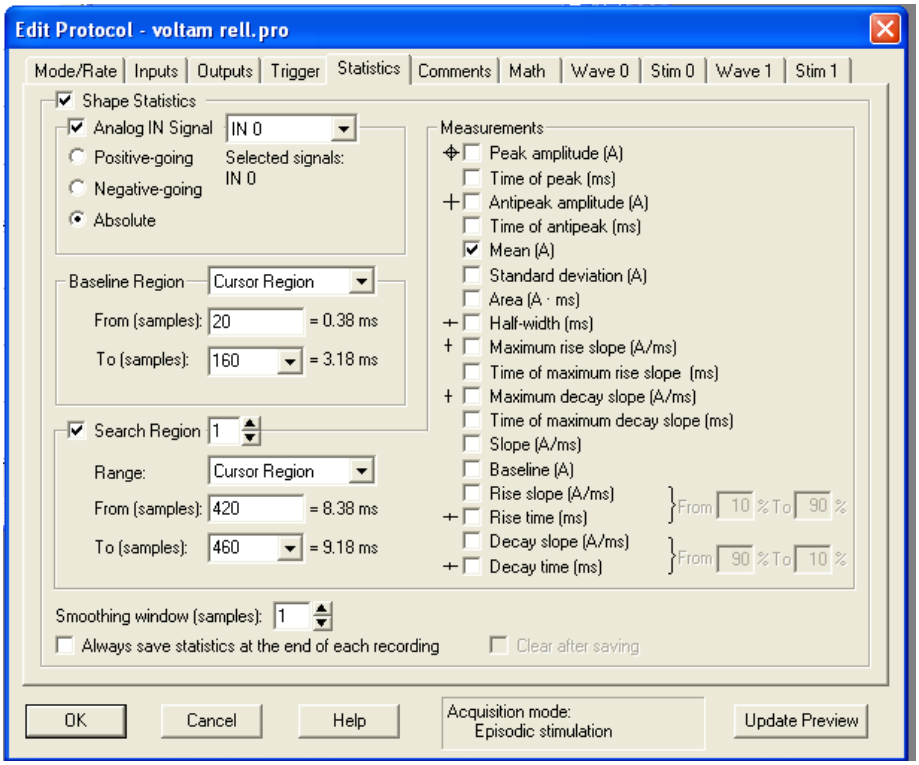
Edit Protocol - voltam rell.pro
Mode/Rate
Inputs
Outputs
Trigger
Statistics
Comments
Math
Wave 0
Stim 0
Wave 1
Stim 1
Shape Statistics
Analog IN Signal
IN 0
Positive-going
Negative-going
Absolute
Selected signals:
IN 0
Baseline Region
Cursor Region
From (samples):
20
= 0.38 ms
To (samples):
160
= 3.18 ms
Search Region
1
Range:
Cursor Region
From (samples):
420
= 8.38 ms
To (samples):
460
= 9.18 ms
Measurements
Peak amplitude (A)
Time of peak (ms)
Antipeak amplitude (A)
Time of antipeak (ms)
Mean (A)
Standard deviation (A)
Area (A · ms)
Half-width (ms)
Maximum rise slope (A/ms)
Time of maximum rise slope (ms)
Maximum decay slope (A/ms)
Time of maximum decay slope (ms)
Slope (A/ms)
Baseline (A)
Rise slope (A/ms)
Rise time (ms)
Decay slope (A/ms)
Decay time (ms)
From 10 % To 90 %
From 90 % To 10 %
Smoothing window (samples):
1
Always save statistics at the end of each recording
Clear after saving
OK
Cancel
Help
Acquisition mode:
Episodic stimulation
Update Preview

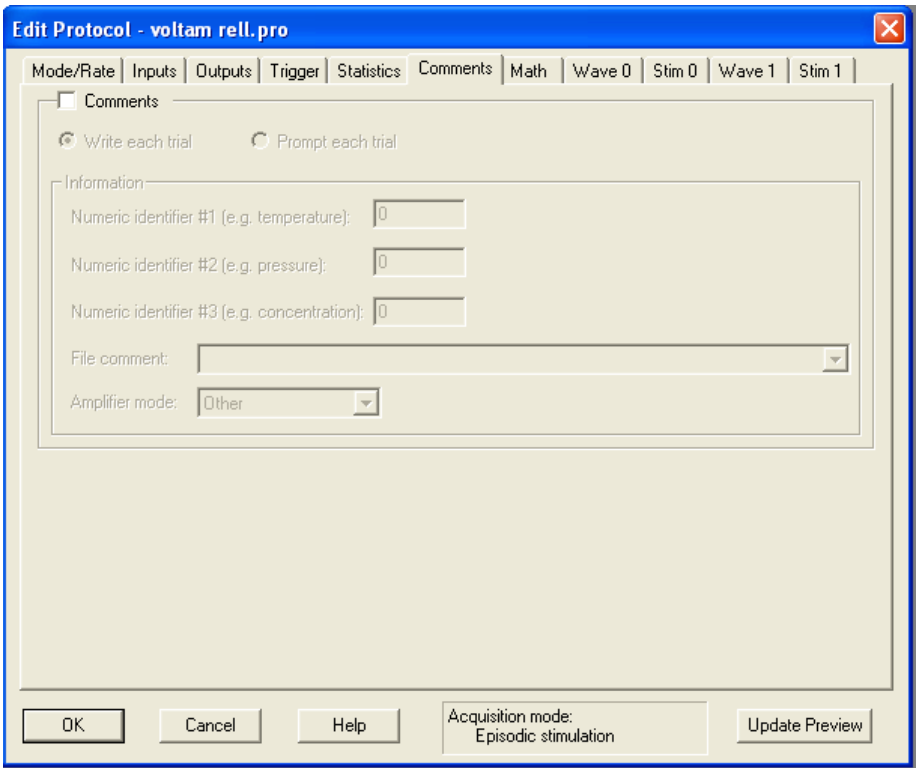
Edit Protocol - voltam rell.pro
Mode/Rate
Inputs
Outputs
Trigger
Statistics
Comments
Math
Wave 0
Stim 0
Wave 1
Stim 1
Comments
Write each trial
Prompt each trial
Information
Numeric identifier #1 (e.g. temperature):
0
Numeric identifier #2 (e.g. pressure):
0
Numeric identifier #3 (e.g. concentration):
0
File comment:
Amplifier mode:
Other
OK
Cancel
Help
Acquisition mode:
Episodic stimulation
Update Preview

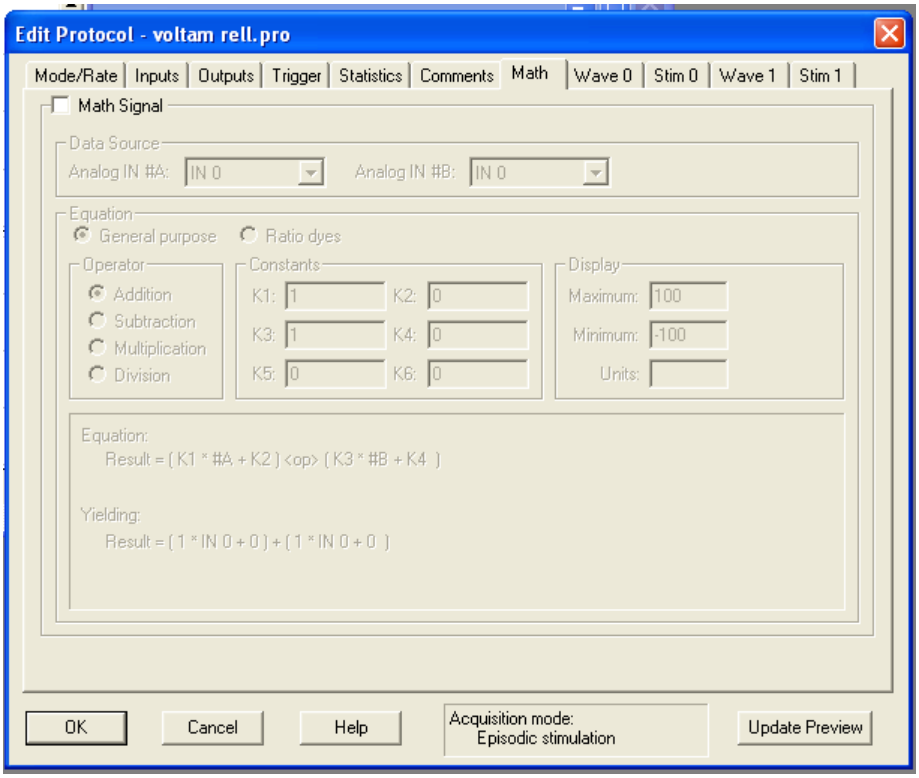
Edit Protocol - voltam rell.pro
Mode/Rate
Inputs
Outputs
Trigger
Statistics
Comments
Math
Wave 0
Stim 0
Wave 1
Stim 1
Math Signal
Data Source
Analog IN #A:
IN 0
Analog IN #B:
IN 0
Equation
General purpose
Ratio dyes
Operator
Addition
Subtraction
Multiplication
Division
Constants
K1:
1
K2:
0
K3:
1
K4:
0
K5:
0
K6:
0
Display
Maximum:
100
Minimum:
-100
Units:
Equation:
Result = (K1 * #A + K2) <op> (K3 * #B + K4)
Yielding:
Result = (1 * IN 0 + 0) + (1 * IN 0 + 0)
OK
Cancel
Help
Acquisition mode:
Episodic stimulation
Update Preview

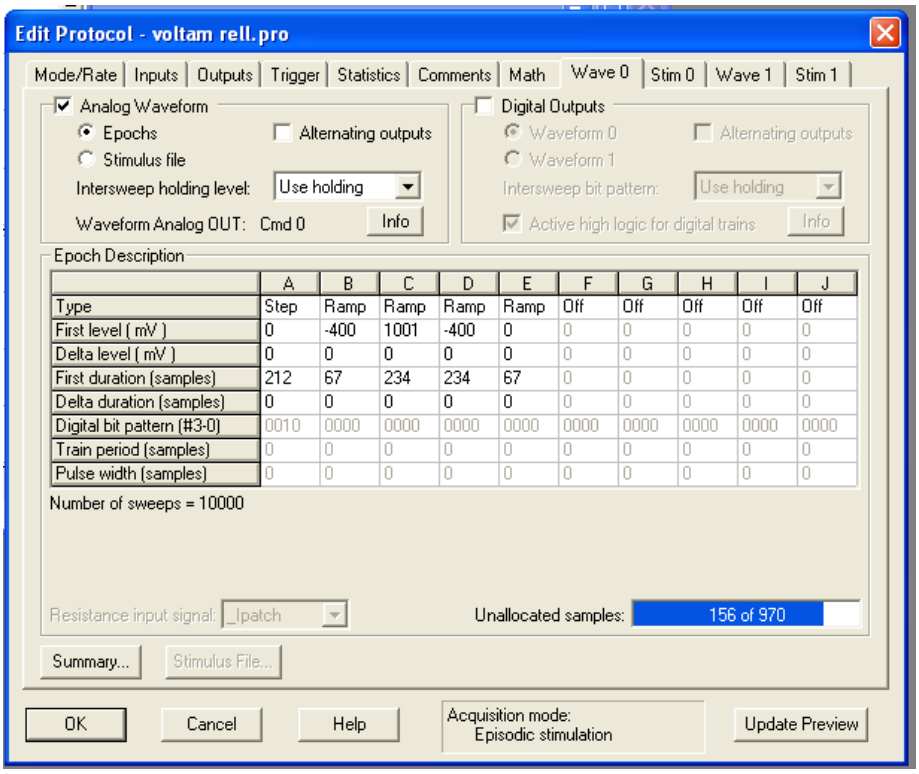
Edit Protocol - voltam rell.pro
Mode/Rate | Inputs | Outputs | Trigger | Statistics | Comments | Math | Wave 0 | Stim 0 | Wave 1 | Stim 1
Analog Waveform
Epochs
Stimulus file
Alternating outputs
Intersweep holding level: Use holding
Waveform Analog OUT: Cmd 0
Info
Digital Outputs
Waveform 0
Waveform 1
Alternating outputs
Intersweep bit pattern: Use holding
Active high logic for digital trains
Info
Epoch Description
A B C D E F G H I J
Type Step Ramp Ramp Ramp Ramp Off Off Off Off Off
First level (mV) 0 -400 1001 -400 0 0 0 0 0 0
Delta level (mV) 0 0 0 0 0 0 0 0 0 0
First duration (samples) 212 67 234 234 67 0 0 0 0 0
Delta duration (samples) 0 0 0 0 0 0 0 0 0 0
Digital bit pattern (#3-0) 0010 0000 0000 0000 0000 0000 0000 0000 0000 0000
Train period (samples) 0 0 0 0 0 0 0 0 0 0
Pulse width (samples) 0 0 0 0 0 0 0 0 0 0
Number of sweeps = 10000
Resistance input signal: _Ipatch
Unallocated samples: 156 of 970
Summary...
Stimulus File...
OK
Cancel
Help
Acquisition mode: Episodic stimulation
Update Preview

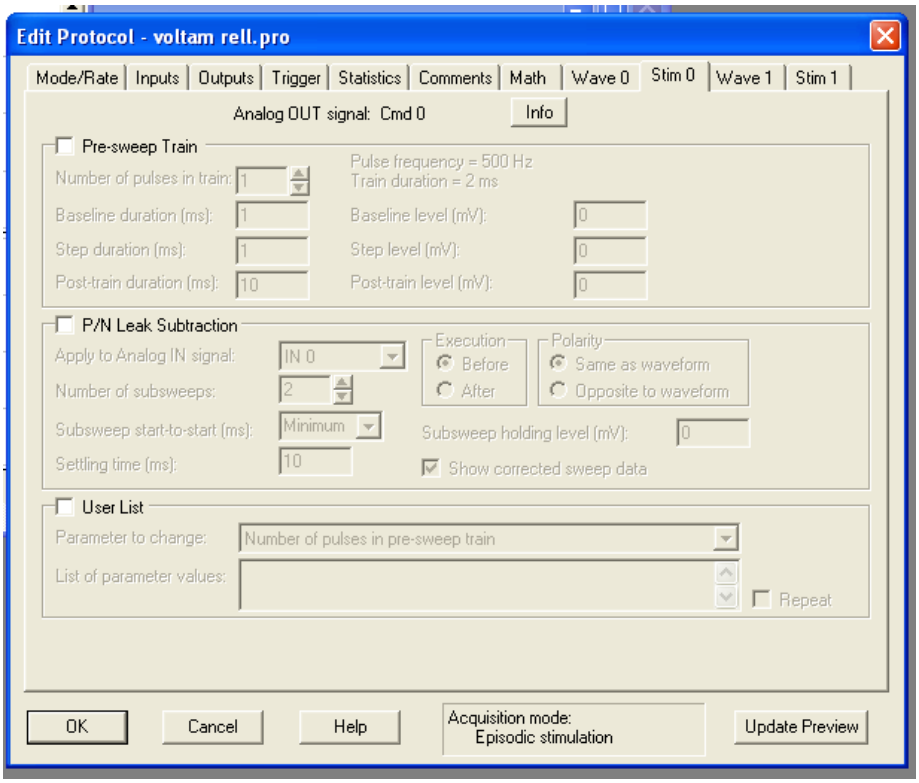
Edit Protocol - voltam rell.pro
Mode/Rate | Inputs | Outputs | Trigger | Statistics | Comments | Math | Wave 0 | Stim 0 | Wave 1 | Stim 1
Analog OUT signal: Cmd 0
Info
Pre-sweep Train
Number of pulses in train: 1
Pulse frequency = 500 Hz
Train duration = 2 ms
Baseline duration (ms): 1
Baseline level (mV): 0
Step duration (ms): 1
Step level (mV): 0
Post-train duration (ms): 10
Post-train level (mV): 0
P/N Leak Subtraction
Apply to Analog IN signal: IN 0
Number of subsweeps: 2
Subsweep start-to-start (ms): Minimum
Settling time (ms): 10
Execution
Before
After
Polarity
Same as waveform
Opposite to waveform
Subsweep holding level (mV): 0
Show corrected sweep data
User List
Parameter to change: Number of pulses in pre-sweep train
List of parameter values:
Repeat
OK
Cancel
Help
Acquisition mode: Episodic stimulation
Update Preview

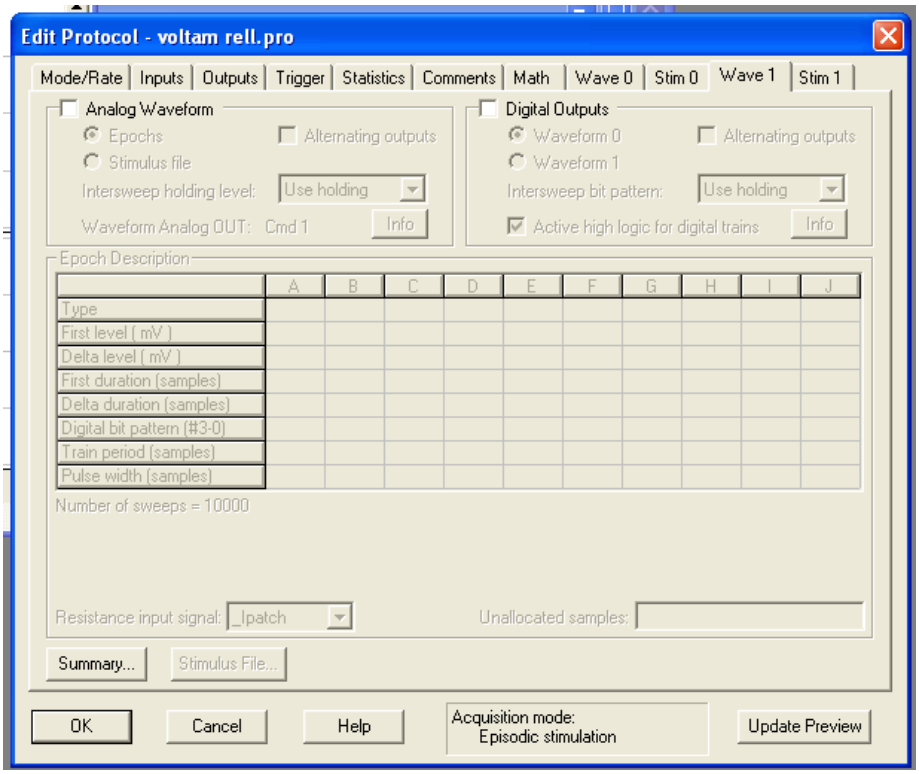
Edit Protocol - voltam rell.pro
Mode/Rate
Inputs
Outputs
Trigger
Statistics
Comments
Math
Wave 0
Stim 0
Wave 1
Stim 1
Analog Waveform
Epochs
Alternating outputs
Stimulus file
Intersweep holding level:
Use holding
Waveform Analog OUT:
Cmd 1
Info
Digital Outputs
Waveform 0
Alternating outputs
Waveform 1
Intersweep bit pattern:
Use holding
Active high logic for digital trains
Info
Epoch Description
A
B
C
D
E
F
G
H
I
J
Type
First level (mV)
Delta level (mV)
First duration (samples)
Delta duration (samples)
Digital bit pattern (#3-0)
Train period (samples)
Pulse width (samples)
Number of sweeps = 10000
Resistance input signal:
_Ipatch
Unallocated samples:
Summary...
Stimulus File...
OK
Cancel
Help
Acquisition mode:
Episodic stimulation
Update Preview

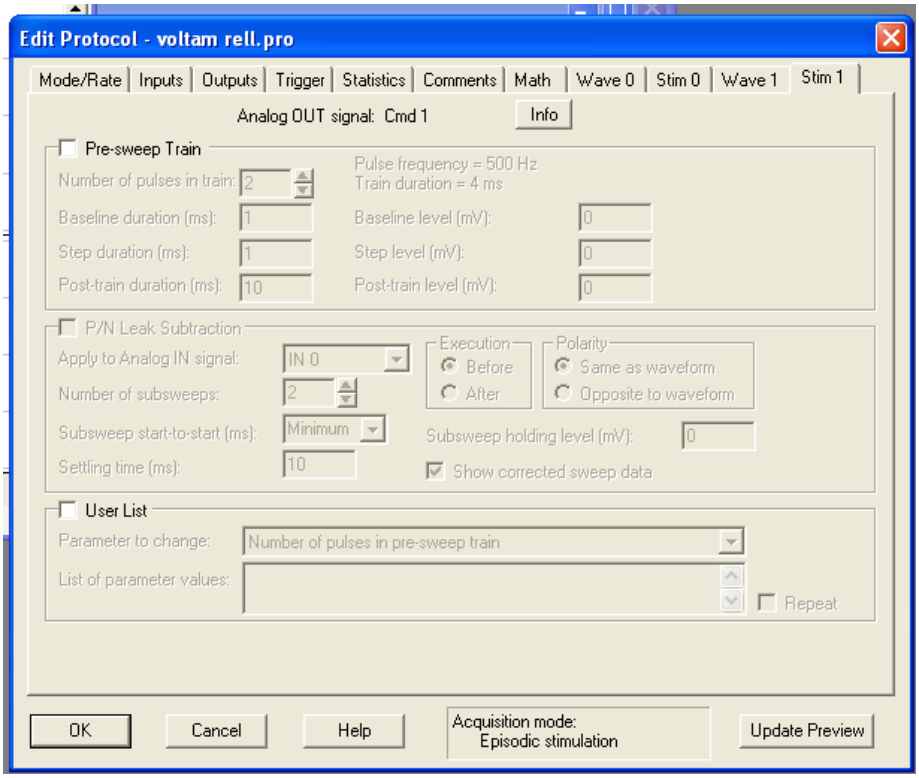
Edit Protocol - voltam rell.pro
Mode/Rate
Inputs
Outputs
Trigger
Statistics
Comments
Math
Wave 0
Stim 0
Wave 1
Stim 1
Analog OUT signal:
Cmd 1
Info
Pre-sweep Train
Number of pulses in train:
2
Pulse frequency = 500 Hz
Train duration = 4 ms
Baseline duration (ms):
1
Baseline level (mV):
0
Step duration (ms):
1
Step level (mV):
0
Post-train duration (ms):
10
Post-train level (mV):
0
P/N Leak Subtraction
Apply to Analog IN signal:
IN 0
Execution
Before
After
Polarity
Same as waveform
Opposite to waveform
Number of subsweeps:
2
Subsweep start-to-start (ms):
Minimum
Subsweep holding level (mV):
0
Settling time (ms):
10
Show corrected sweep data
User List
Parameter to change:
Number of pulses in pre-sweep train
List of parameter values:
Repeat
OK
Cancel
Help
Acquisition mode:
Episodic stimulation
Update Preview